

AD-A101 983

NAVAL RESEARCH LAB WASHINGTON DC  
PERFORMANCE OF THE SOLAR CELL EXPERIMENTS ABOARD THE NTS-2 SATE--ETC(U)  
JUL 81 D H WALKER.

F/G 10/2

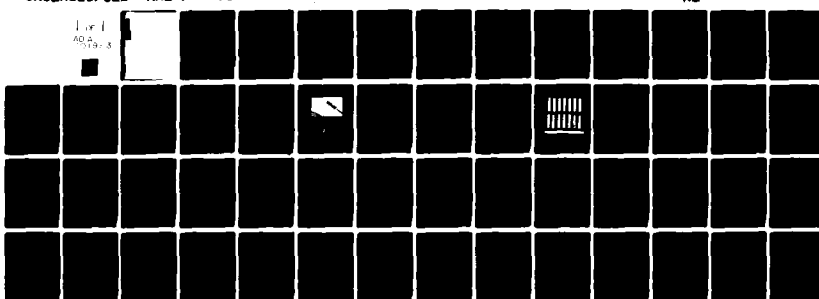
DATE--ETC(U)

UNCLASSIFIED

NRL-MR-4580

NL

1 or 1  
AD-A101 983



END  
DATE  
FILED  
8-81  
DTIC

AD A101983

SECURITY CLASSIFICATION OF THIS PAGE (When Data Entered)

REPORT DOCUMENTATION PAGE		READ INSTRUCTIONS BEFORE COMPLETING FORM	
1. REPORT NUMBER NRL Memorandum Report 4580	2. GOVT ACCESSION NO. AD-A102 983	3. RECIPIENT'S CATALOG NUMBER	
4. TITLE (and Subtitle) PERFORMANCE OF THE SOLAR CELL EXPERIMENTS ABOARD THE NTS-2 SATELLITE AFTER THREE YEARS IN ORBIT	5. TYPE OF REPORT & PERIOD COVERED Interim report from 1 October 1979 to 30 September 1980.		
7. AUTHOR(s) D. H. Walker	6. PERFORMING ORG. REPORT NUMBER		
9. PERFORMING ORGANIZATION NAME AND ADDRESS Naval Research Laboratory Washington, D.C. 20375	10. PROGRAM ELEMENT, PROJECT, TASK AREA & WORK UNIT NUMBERS 61153N; RR0120141; USAF 62203F; 66-0411-0 & 66-0415-0		
11. CONTROLLING OFFICE NAME AND ADDRESS	12. REPORT DATE July 30, 1981		
14. MONITORING AGENCY NAME & ADDRESS (if different from Controlling Office)	13. NUMBER OF PAGES 54		
16. DISTRIBUTION STATEMENT (of this Report) Approved for public release; distribution unlimited.	15. SECURITY CLASS. (of this report) UNCLASSIFIED		
17. DISTRIBUTION STATEMENT (of the abstract entered in Block 20, if different from Report)	18. DECLASSIFICATION/DOWNGRADING SCHEDULE		
19. SUPPLEMENTARY NOTES			
19. KEY WORDS (Continue on reverse side if necessary and identify by block number) Solar cells Space radiation Solar cell coverslips Satellite power systems			Radiation damage I-V curve NTS-2 Photovoltaic cells
20. ABSTRACT (Continue on reverse side if necessary and identify by block number) This report presents the results obtained from the solar cell experiment aboard the NTS-2 satellite after 1,176 days in orbit. The objective of the solar cell experiment is to evaluate the performance and radiation hardness of state-of-the-art solar cells in the space environment. The experiment is comprised of fifteen (15) separate experimental modules each containing five 2 X 2 cm solar cells connected in series. The solar cell types include advanced state-of-the-art silicon solar cells such as the COMSAT CNR cell, the Spectrolab Textured Helios Reflector cell, and the Solarex Vertical Junction cell. Also included for the first time in a flight experiment is the Hughes gallium-arsenide/gallium-			(Continues)

## 20. ABSTRACT (Continued)

aluminum-arsenide cell. There are also on board experiments to evaluate environmental effects on coverslip adhesives.

Telemetered data indicate a radiation environment in the 63 degree, 21,190 km circular orbit of NTS-2 only slightly harder than the predicted value for 1 MeV electron fluence equivalent calculated from space radiation models. Based on the NTS-2 data, the spacecraft main solar array of Spectrolab Helios cells had degraded 32 percent in maximum power over the intended three-year mission. Solar cell temperatures have reached 105 degrees C, providing the opportunity to look for moderate temperature annealing of radiation-induced damage in the gallium arsenide cells.

After more than three years in orbit, the loss in power ranged from 24.2 percent in the Spectrolab Textured Hybrid cell with FEP Teflon bonded coverslip to 56.1 percent in the COMSAT textured cell without uv filter. These values do not include the following three solar cell modules which have ceased to function: (1) the Solarex space cell (exp. 8) which became open-circuited on the 69th day; (2) the Solarex vertical junction cell (exp. 7) which failed on day 720; and (3) the Spectrolab Textured Helios Reflector cell (exp. 9) which failed on day 783. The average value of solar simulator  $I_{sc}$  agrees to within  $1.41 \pm 0.99$  percent of the value measured in space. The agreement between  $V_{oc}$  in space and solar simulator values was  $1.24 \pm 1.08$  percent. The changes in the photovoltaic parameters of each of the experiments are summarized in the report.

Accession For	
NTIS CRA&I	<input checked="" type="checkbox"/>
DTIC TAB	<input type="checkbox"/>
Unannounced	<input type="checkbox"/>
Justification	
By	
Distribution/	
Availability Codes	
Avail and/or	
Dist	Special

## CONTENTS

BACKGROUND .....	1
REQUIREMENTS .....	2
EXPERIMENTAL RESULTS .....	3
RADIATION ENVIRONMENT .....	11
CONCLUSIONS .....	12
ACKNOWLEDGMENTS .....	13
REFERENCES .....	50

PERFORMANCE OF THE SOLAR CELL EXPERIMENTS ABOARD  
THE NTS-2 SATELLITE AFTER THREE YEARS IN ORBIT

Background

It is becoming increasingly important in these days of greater dependence on satellite systems for our nation's defense, communications, and economy, that spacecraft systems be designed for complex operations using components which possess high efficiencies and long lifetimes. Nowhere is this more critical than with the solar cells that provide electrical power for satellites. The duration of each satellite mission is determined mainly by the functional lifetimes of the solar cells that power it.

The Navigation Technology Satellite-Two (NTS-2) is the second in a series of developmental satellites that are precursors of the DoD NAVSTAR Global Positioning System (GPS). NAVSTAR GPS is being developed as a constellation of satellites that will use passive ranging techniques combined with highly accurate clocks to provide extremely accurate navigation capability to ships, aircraft, ground forces, and other users 24 hours a day, worldwide, in any kind of weather. The GPS satellites occupy various positions in orbit, thereby affording extremely accurate three-dimensional navigational information, i.e., longitude, latitude, and altitude. NTS-2 was launched 23 June 1977 into a twelve-hour circular orbit 20,192 km high at an inclination of 63°.

In support of the Global Positioning Satellite System, fifteen state-of-the-art solar cell modules were flown on the NTS-2 satellite. The purpose of the experiments is to measure the radiation resistance and the effects of the space environment on the degradation rates of the photovoltaic parameters of these solar cells throughout the flight. The initial space performance will also be compared with prelaunch ground

performance. Although numerous attempts at measuring radiation and other space environmental effects on solar cells have been made in the laboratory,<sup>1-10</sup> it is difficult, if not impossible, to duplicate the combined effects the solar cells will actually experience in a given orbit. Such environmental factors as the proper ratio of electron to proton fluence, the exact temperature profile that will be encountered, and the correct type of ultraviolet radiation are not easily simulated. For the above reasons, the importance of solar cell flight experiments such as those flown on the NTS-2 satellite cannot be overstated. Flight experiments afford the opportunity to measure radiation and other environmental effects in situ. Test and evaluation under these conditions remain the most meaningful way to determine which state-of-the-art solar cells meet our future requirements.

These experiments will also answer questions that have arisen from the NTS-1 solar cell flight experiments,<sup>11-13</sup> such as: the need for ultraviolet rejection filters in space solar cell systems, space qualification of electrostatic bonding techniques for solar cell coverslips, and the improved efficiency to be realized from the use of textured cell surfaces. In addition, a gallium arsenide (GaAlAs/GaAs) solar cell module is being flight tested. Each of the fifteen (15) separate experiments consists of an array of five 2 cm x 2 cm state-of-the-art solar cells. The experiments are linked to an electronics circuit which measures the entire photovoltaic I-V curve of each experiment in sequence every two minutes.

#### Requirements

This is the third annual report on the NTS-2 solar cell flight experiments, covering the period from 1 October 1979 through 30 September 1980.

The major goals of the past year's work at the Naval Research Laboratory were to reduce, correct, and analyze the data to provide a history of the temperature, open-circuit voltage, short-circuit current and maximum power for all fifteen experiments. These goals have been achieved. Some of the results have been published

in interim reports. The results of the NTS-2 solar cell flight experiments from launch through 30 September 1980 are summarized in detail in this report.

#### Experimental Results

This report covers the analysis of data from the fifteen (15) solar cells from forty-eight (48) orbital revolutions, covering 1,176 days in orbit. The NTS-2 satellite was launched 23 June 1977 from the Western Test Range at Vandenberg AFB. Fourteen days later, the space craft had been stabilized and the solar power panels were deployed, allowing the solar cell experiments their first exposure to solar illumination and to the total space radiation environment. That date, 7 July 1977, is counted as day one in this report. Prior to deployment, the main solar power panels remained in the wrap-around launch configuration as shown in Fig. 1a. This arrangement provided a cover for the solar cell experiments with an effective shielding thickness of 40 mils of aluminum ( $0.274 \text{ gm/cm}^2$ ). During its orbit, the satellite is rotated around the appropriate axis as needed to maximize the solar cell paddle exposure to the sun. Because of the location of the experiments, this maneuver also maximizes the exposure of the experiments to the sun. Figure 1b shows the location of the panels on the spacecraft.

The current-voltage (I-V) characteristics of the solar cell arrays are telemetered in real time as the satellite passes over the tracking station at Blossom Point, Maryland. The electronic circuit shown in Fig. 2, measures the I-V curve for each module in sequence reading out current-voltage values for evenly-spaced points from short-circuit current ( $I_{sc}$ ) to open-circuit voltage ( $V_{oc}$ ) every two minutes. A typical I-V curve showing the number and spacing of points obtained is shown in Fig. 3. Each cell module is short-circuited except when it is being stepped through the I-V curve. The first data were obtained from the experiments within 6 hours of deployment. During the first revolution recorded after deployment the panel temperature measured close to  $60^\circ\text{C}$ .

Temperatures are monitored at the rear surface of four cells by means of three thermistors and one wire resistance thermometer. The thermistors are accurate to within  $\pm 3$  degrees C up to  $100^{\circ}\text{C}$ , and the wire thermometer is accurate to within  $\pm 2$  degrees C to above  $120^{\circ}\text{C}$ . The experimental panels are continuously illuminated by the sun (except during the biannual eclipse season of 25 days) by virtue of the sun orientation requirements of the main array.

Since day 1, the panel temperatures have gradually increased to higher than  $100^{\circ}\text{C}$ . Since September 1978, the temperatures have remained stable. The solar cells on panel 1 maintain a temperature around  $105^{\circ}\text{C}$  while the temperature of the solar cells on panel 2 is near  $100^{\circ}\text{C}$ . The temperatures of both solar cell panels versus days in orbit are shown in Fig. 4. This temperature rise in excess of 20 degrees higher than predicted has been attributed to the ultraviolet and particle radiation degradation of the white silastic thermal control coating, DC 92007, that covers all panel areas surrounding the solar cell modules. The coated area totals 52 percent of the panel's surface. A closeup view of the panel is shown in Fig. 5. It is possible that exposure to ultraviolet and particle radiation has increased the solar thermal absorptivity ( $\alpha_s$ ) of the thermal control coating from 0.27 to a higher value, which would account for the higher temperatures. Table I gives a brief description of the experiments, showing the type and thickness of the solar cell, the type and thickness of the coverslip, the nature of the coverslip-to-cell bonding, the interconnect material, and the beginning-of-life (BOL) cell efficiency.

The first  $I_{\text{sc}}$  and  $V_{\text{oc}}$  data measured in space were in good agreement with the ground calibrations which were done at NRL and Air Force Aero Propulsion Laboratory (AFAPL). The data have been corrected for solar intensity (day of the year), for solar aspect angle and to a cell temperature of  $50^{\circ}\text{C}$ . The average spread in  $I_{\text{sc}}$  between NRL and AFAPL was only 2 mA; the average of these measurements is used as the ground calibration numbers reported here. The solar cells that comprise the NTS-2

flight experiment were measured at NRL prior to launch under solar simulator conditions. An RAE standard cell provided by the Royal Aircraft Establishment, Farnboro, England, was used to make the prelaunch calibrations at NRL. The standard cell was a 10 ohm-cm Ferranti cell that had been calibrated on the ground at Malta in 1973. The average error between  $I_{sc}$  on the first day in space and the pre-flight values is  $1.412 \pm 0.99$  percent. The difference between  $V_{oc}$  in space and solar simulator values is  $1.24 \pm 1.08$  percent. These are much more accurate results than were obtained for the NTS-1 solar cell experiment.<sup>13</sup> The initial NTS-1 experiment  $I_{sc}$  data deviated from the ground calibration values by as much as 15 percent for some modules. The average error between maximum power ( $P_m$ ) measurements on the ground and the first day in orbit was  $3.33 \pm 3.17$  percent. The greatest difference was for the gallium arsenide cell, where the difference was 12.3 percent. It is not possible that this is entirely a measurement error, but it is believed there was a possibility for physical change in the cell module in the time between the last ground calibration with a solar simulator and the space measurement 145 days later. The GaAs cell module subsequently showed a significant amount of  $P_m$  and  $V_{oc}$  recovery after 80 days in space (see Fig. 6).

Four experiments have either failed completely or sustained unpredictably large degradations. The first of these, the Solarex Low Cost Space Cell, Experiment 8, experienced an open-circuit of the module on the 69th day, causing the complete loss of subsequent data. Fortunately this failure occurred while data were being recorded, allowing the abrupt manner in which it failed to be observed. The suddenness of the failure is shown in Fig. 7. Analysis of the data acquisition system showed that no single-point failure of the data system could result in both voltage and current data loss. Therefore it is presumed the module open-circuited.

A second anomaly was the sudden onset of increased degradation rate in the Solarex vertical junction cell, Experiment 7 (Fig. 8). There were a total of five sudden

drops in the maximum power output of the vertical junction cells. These sharp decreases occurred around day 20 in orbit, close to day 180, between day 365 and day 390, and near day 560. The onset of the fifth event occurred about day 729. However, due to subsequent failure of the module no further data were received. The decrease in the maximum power output of the vertical junction cells was 70.7 percent on day 729. Evidence of their impending failure was seen during the revolution recorded on that date. The data received were intermittent, i.e. an I-V curve was not produced for every scan made during that revolution. Investigations directed by the AFAPL<sup>14</sup> suggest that these unusually large losses in maximum power are the result of cell junction disintegration occurring during the thermal cycling of adhesively bonded-coverslipped cells. The data in Fig. 9 seem to support this hypothesis. The abnormal drops in power occur at approximately the same time as the maximum in the daily duration of the eclipse. As the cells cool to lower temperature, the stress at the cell-coverslip interface due to thermal coefficient mismatch becomes more severe, destroying some of the cell junction. The effect is a loss in cell power. The breakdown of the junction may be related to the type of adhesive used to bond the coverslip. Following each drop in  $P_m$  prior to the total failure, the power output was normally predictable until the next maximum daily duration of the eclipse period.

The Spectrolab textured Helios reflector cells comprising Experiment 9 have also ceased to transmit data. The last data were received on day 721; by the time the next data were received on day 783, there was no output from Experiment 9. Prior to day 783, there had been no indication of any malfunction. The data from Experiment 9 are shown in Fig. 10.

Another unusual occurrence is the large degradation rate for Experiment 5, the COMSAT textured cell covered with a 12 mil (0.305 cm) fused silica coverslip which has no ultraviolet cut-off filter. The coverslip adhesive is R63-489. The COMSAT textured cell was flown both with and without an ultraviolet rejection filter on the coverslip in

order to evaluate the effect of the filter. The maximum power ( $P_m$ ) of this cell has decreased 56.1 percent down to 32.8 mW after 1,176 days, while Experiment 6, an identical module except for the addition of the ultraviolet cut-off filter on the coverslip, has a remaining  $P_m$  of 48.1 mW, a drop of only 33.2 percent. A comparison between the short-circuit current loss in the two COMSAT modules shows the dramatic effect of removing the uv filter. Although the two arrays started with nearly the same beginning-of-life (BOL) short-circuit current, the  $I_{sc}$  of the cells with the uv filter (Experiment 6) has degraded only 29.2 percent. However, the  $I_{sc}$  of Experiment 5 without the uv filter decreased by 49.4 percent. Figure 11 shows the short-circuit current degradation of the COMSAT textured cell in both configurations. This amount is much greater than was predicted. Previous experiments indicated that degradation from ultraviolet degradation of the solar cell assembly is about 2 to 4 percent. This damage was believed to occur and stabilize during the first few weeks in space. In fact, laboratory measurements at COMSAT Laboratories did not show a substantial difference with or without a filter.<sup>15</sup> If we hypothesize that the degradation seen in the  $I_{sc}$  of these cells were caused by particle radiation in the cell, the  $V_{oc}$  would also be greatly degraded. But Fig. 12 shows that the  $V_{oc}$  of the cells with and without the uv filter is essentially the same. Neither the fill factor of Experiment 5 nor the knee of its I-V curve, which would be noticeably "softened," show any effects from radiation damage. Even at this time, the reason for the unexpectedly large degradation of the non-filtered cell remains unknown. The effect may involve an unidentified damage mechanism associated with the adhesive or cell antireflective coating. The flight data for Experiments 5 and 6 are shown in Fig. 13 and Fig. 14, respectively. Those modules remaining continue to operate as expected although degrading more rapidly than predicted from the published reports.<sup>16,17</sup> Table II lists the  $P_m$  of the experiments at BOL and after 1,176 days in orbit.

The modules that comprise Experiments 3 and 4 were designed to evaluate a new

method of attaching coverslips to cells. The bonding material is 2-mil-thick FEP Teflon which is laminated between the fused silica and the cell surface. In this technique developed by Spectrolab, bonding is accomplished by the simultaneous application of moderate heat and pressure. In the NTS-2 experiment, the Spectrolab textured hybrid cell was used in the two modules which were constructed with different coverslip systems: Module No. 3 had a 6 mil Corning 7940 fused silica coverslip with ultraviolet filter bonded with DC93-500; module No. 4 had a 6 mil Corning 7940 fused silica "as-sawn" coverslip (no filter or antireflective coating) bonded to the cell with FEP Teflon. "As-sawn" means that the fused silica is not given an optical polish. The I-V data after 941 days show the  $I_{sc}$  loss in the adhesive system to be 24.0 percent compared to only 16.1 percent loss in the FEP Teflon system. The I-V curves on days 1 and 941 are shown in Fig. 15. A plot of  $I_{sc}$  vs. time in orbit for these two modules is given in Fig. 16. It is apparent that the difference in  $I_{sc}$  for the two modules becomes larger with longer time in orbit. This indicates that adhesive darkening may continue to intensify over a long period of time, contrary to previous belief that the darkening reached a maximum value after only a few weeks or months. The NTS-2 results indicate this effect does not level off, even after more than three years. See Figs. 17 and 18 for the degradation of the photovoltaic parameters vs time in orbit for Exps. No. 3 and No. 4.

Another coverslip evaluation is made in Experiments 1 and 13 which utilize OCLI conventional cells. Experiment 1 has an adhesively bonded Corning 7940 fused silica coverslip and Experiment 13 has a DOW Corning 7370 glass coverslip which was electrostatically bonded (ESB). There was a slight loss in beginning of life  $P_m$  with the electrostatic bonding technique. The power loss after 1,176 days in orbit is only 24.8 percent for the ESB cell compared to 37.8 percent  $P_m$  loss in the adhesively bonded cell. These results are shown in Figs. 19 and 20.

The OCLI conventional cells also provided a baseline to show the improvements in

the advanced cells. The OCLI conventional cell is a typical deep-junction 10 ohm-cm cell, in which the diffused junction is about  $0.5\text{ }\mu\text{m}$  deep. Advanced design cells have junctions in the range of 0.15 to  $0.30\text{ }\mu\text{m}$ . Figure 21 clearly shows the gain in power afforded by the newer cells, such as the OCLI Violet, the Helios, and the Spectrolab Textured Hybrid. At 1,176 days the power output of the advanced cells was higher by 15 to 35 percent. Figure 21 also shows the interesting fact that the slope of the power degradation curve of the Textured Hybrid cell is much less than that for the other cells. This Hybrid cell module is the one utilizing FEP Teflon as the coverslip bonding medium, while the other modules shown here use an adhesive system.

An (AlGa)As-GaAs solar cell with a 12 mil 7940 fused silica coverslip and DC93-500 adhesive comprises Experiment 15. This module, which was made by the Hughes Research Laboratory, had an efficiency of 13.6 percent. These cells have a junction depth of 1 micron, and are interconnected by a metal-filled epoxy. The historical problems of high surface recombination and low lifetime in the diffused region of GaAs are largely overcome by the addition of a GaAlAs window. These cells, which were expected to be radiation hardened and therefore be especially suited to space applications, behaved in a very unusual manner during the first 3 months. The GaAs cells sustained a sharp drop in power output as measured on the first orbit and throughout the next 28 days as shown in Fig. 6. The  $P_m$  gradually increased to its peak value on the 100th day, then the normal rate of radiation degradation became dominant. The behavior during the early days has not been positively explained; it may be related to the instability of epoxy interconnect material, rather than another identifiable mechanisms in the cell itself.

The degradation in  $I_{sc}$ ,  $V_{oc}$  and  $P_m$  of the GaAs cells versus days in orbit are shown in Fig. 6. The gallium arsenide module at first exhibited the slowest rate of power loss; while no longer the case, after 1,176 days its power had decreased by only 29.6 percent.

The maximum power degradation of the gallium arsenide cell is shown in Fig. 21 along with the highest output cell, the COMSAT nonreflective cell, and with the Spectrolab Helios cell, referred to as the "K-6" cell. The Helios cell is a shallow junction, polished surface, back surface field cell. The fourth cell on the figure is a p/n lithium-doped cell from the 1972 period when there was a concerted effort to develop a radiation hardened solar cell. Lithium was observed to enhance room temperature annealing of radiation induced defects in p/n silicon cells. The annealing was observed to be more prominent in the case for proton damage than for electron damage. Hence the NTS-2 results shown here are somewhat surprising, in that the power output of this cell is nearly as high as the power of the Helios cell after 1,176 days (equivalent to  $10^{15}$  1-MeV e/cm<sup>2</sup>).

The Spectrolab Helios back field cells which comprise Experiment No. 2 are of particular importance. The Helios cell design was space qualified as one of the experiments flown on the NTS-1 satellite. The Helios cells are presently in use as the main power source on NTS-2 and are in use in other satellite programs as well. As of day 1,176 the maximum power output of the Spectrolab Helios cells (NTS-2) has decreased by 34.2 percent. The maximum power plotted versus time in orbit for this module is shown in Fig. 22. Interestingly, although the Helios cells have degraded less than a conventional cell in  $I_{sc}$  and  $P_m$ , its  $V_{oc}$  output continues to degrade at a faster rate. The conventional cells show a  $V_{oc}$  decrease of only 8.2 percent compared to a 12.6 percent degradation in the Helios cell.

Experiments II and I2 were designed to evaluate the performance of a diode in series with solar cells in the space radiation environment. The data from Experiment II and Experiment I2 through 1,176 days in space are shown in Figs. 23 and 24, respectively. As shown in Fig. 25, the voltage drop across the diode had not changed significantly over the first 811 days in space.

The Spectrolab HESP cells, Experiment 14, have degraded in  $P_m$  33.5 percent in  $P_M$ , as shown in Fig. 26.

The maximum power outputs for all of the modules at BOL and after 1,176 days are compared in the bargraph in Fig. 27. The absolute values and percent changes of short-circuit current and open-circuit voltages are listed in Tables III and IV. The percent changes in  $I_{sc}$ ,  $V_{oc}$  and  $P_m$  are summarized in Table V.

#### Radiation Environment

The observed degradation rates of the NTS-2 solar cell experiments were utilized to estimate equivalent 1-MeV electron fluence in the 11,000 nm circular orbit. Prior to launch, an estimation of the equivalent fluence based on the AEI-7 LO electron model which was generated by the National Space Science Data Center gave a value of  $2 \times 10^{14}$  electrons/cm<sup>2</sup>-yr for a solar cell with a 0.030 cm fused silica coverglass.

By day 200, the solar cell experiments had experienced sufficient radiation damage to allow predictions of future damage rates to be made. The fluence of equivalent 1-MeV electrons/cm<sup>2</sup> experienced by four (4) selected groups of solar cells (Experiment 3, the Spectrolab textured hybrid cell; Experiment 1, the OCLI conventional cell; Experiment 2, the Spectrolab Helios cell; and Experiment 10, the OCLI violet cell) by day 200 is tabulated in Table VI. These data were used to predict the estimated annual fluence and the fluence expected over 3 years. The corrected space data for these experiments through day 1,176 are shown in Figs. 17, 19, 21 and 28, respectively. The OCLI 2 ohm-cm cell is used as a reference because the effects of varied amounts of fluence on these cells have been studied extensively over the past decade. The predicted degradation rate of  $P_m$  calculated from these experiments for the first three years in orbit is plotted in Fig. 29 along with the experimental data from the Helios cells. The flight data indicate the presence of a slightly harder radiation environment than was predicted. The relative degradations of the cells mentioned above, as calculated for day 200, and predicted for 1 year and 3 years, are shown

in Table VII. On day 1,176 the  $P_m$  of each of the experiments was approximately 2.5 percent lower than predicted. The degradation curves for these four modules, Experiments 1, 2, 3, and 10 were compared with laboratory results of 1-MeV electron irradiation tests of similar cells. From these data we obtained values for DENI space fluence of  $1.6-2.7 \times 10^{14}$  1-MeV electron/cm<sup>2</sup> year.

Using the most recent  $I_{sc}$  and  $P_m$  degradation rates in space, and comparing these data with published data from ground tests of similar cells, we have obtained a value of approximately  $3.4 \pm 0.8 \times 10^{14}$  1-MeV electrons/cm<sup>2</sup>-yr. We have observed that most of the  $V_{oc}$  data do not indicate this high a fluence, but more nearly  $1.5 \times 10^{14}$  e/cm<sup>2</sup>-yr for a 0.030 cm fused silica coverglass. As pointed out by H.Y. Tada and J.R. Carter, Jr.,<sup>17</sup> the trapped proton fluence is negligible in this orbit as are the solar flare protons thus far. Our empirical value is based on fitting data from Exps. 1, 2, 3, 4, 10, and 13 to degradation curves in Ref. 18. We have subtracted power loss in the modules which can be attributed to adhesive and coverslip darkening in order to arrive at an equivalent fluence pertaining to cell damage only.

#### Conclusions

The following conclusions can be drawn after observing more than three years of orbital performance:

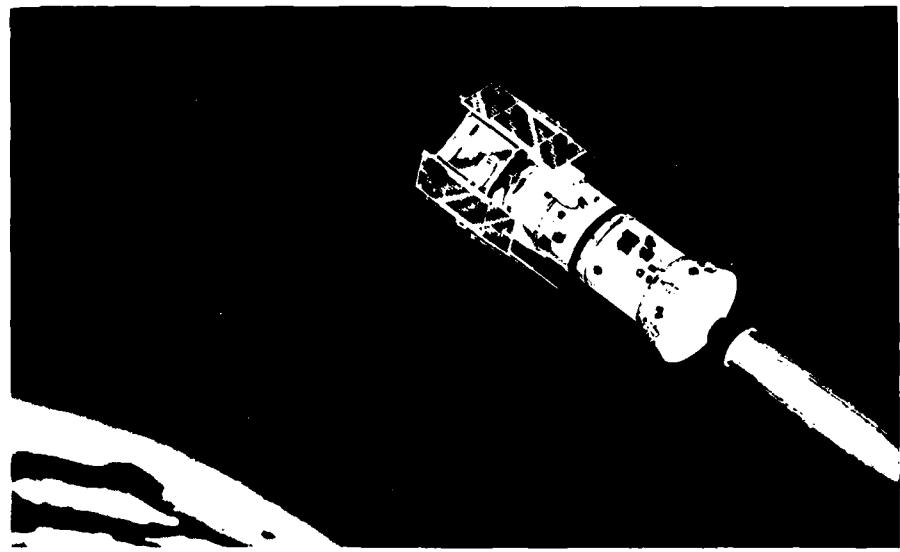
- (1) The NTS-2 solar cell experiments continue to operate successfully and to transmit valuable data.
- (2) The effect of the trapped electron environment at 11,000 nm, 63° inclination orbit on silicon solar cells can be fairly well predicted by multiplying the equivalent 1-MeV fluence obtained from the NNDC AEI-7 model by a factor of two.
- (3) The Spectrolab Helios p<sup>+</sup> (K6) cell with an adhesively-bonded 10 mil (0.0254 cm) ceria microsheet coverslip is an excellent solar

cell for operating in the natural space environment of the GPS orbit. The Spectrolab textured hybrid cell with an FEP bonded 6 mil (0.0152 cm) "as-cut" quartz coverslip seems to be equally satisfactory for this orbit

- (4) The total loss in  $P_m$  for production type silicon cells varies from a high of 37.8 percent in a 10.7 percent efficient conventional two ohm-cm cell with adhesively bonded 12 mil silica cover to 22.6 percent loss in a 11.1 percent efficient textured shallow-junction cell with an FEP bonded 6 mil silica cover. The losses reported here do not include 40.8 percent loss exhibited by experiment No. 5 due to lack of uv filter.
- (5) The highest remaining power output in an experimental solar cell is in the COMSAT Nonreflecting cell with an initial efficiency of 14.6 percent, covered with adhesively bonded 12 mil fused silica. This cell retained 66.8 percent of initial power after an equivalent fluence of  $10^{15}$  1-MeV e/cm<sup>2</sup>.
- (6) The (AlGa)As-GaAs cell with a 1 micron junction depth maintains good power output at 43.2 mW, being surpassed only by the COMSAT Nonreflecting cell (Exp. 6) at 48.1 mW and the OCLI violet cell at 46.0 mW.

#### Acknowledgments

The author expresses appreciation to R.L. Statler for suggestions and assistance, to Dr. K.W. Marlow, Head of the Radiation Survivability and Detection Branch, to J. Wise, Air Force Aero Propulsion Laboratory, and to CAPT R. Widby, Space Division, Air Force Systems Command, for their continual support; and to R. J. Lambert of the Radiation Detection Section for his help with the data reduction.



78411

Fig. 1a — The NTS-2 satellite with solar paddles folded during launch

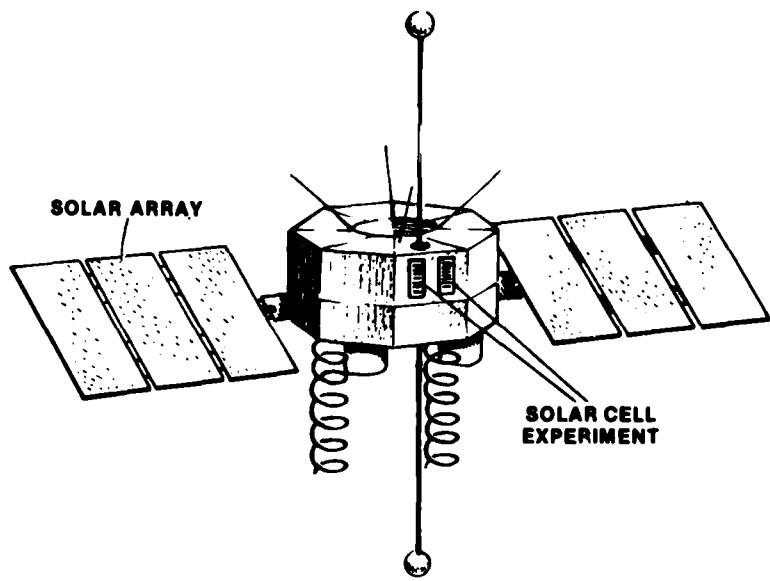


Fig. 1b — The NTS-2 satellite with solar arrays deployed and showing the location of the two solar cell experiment panels

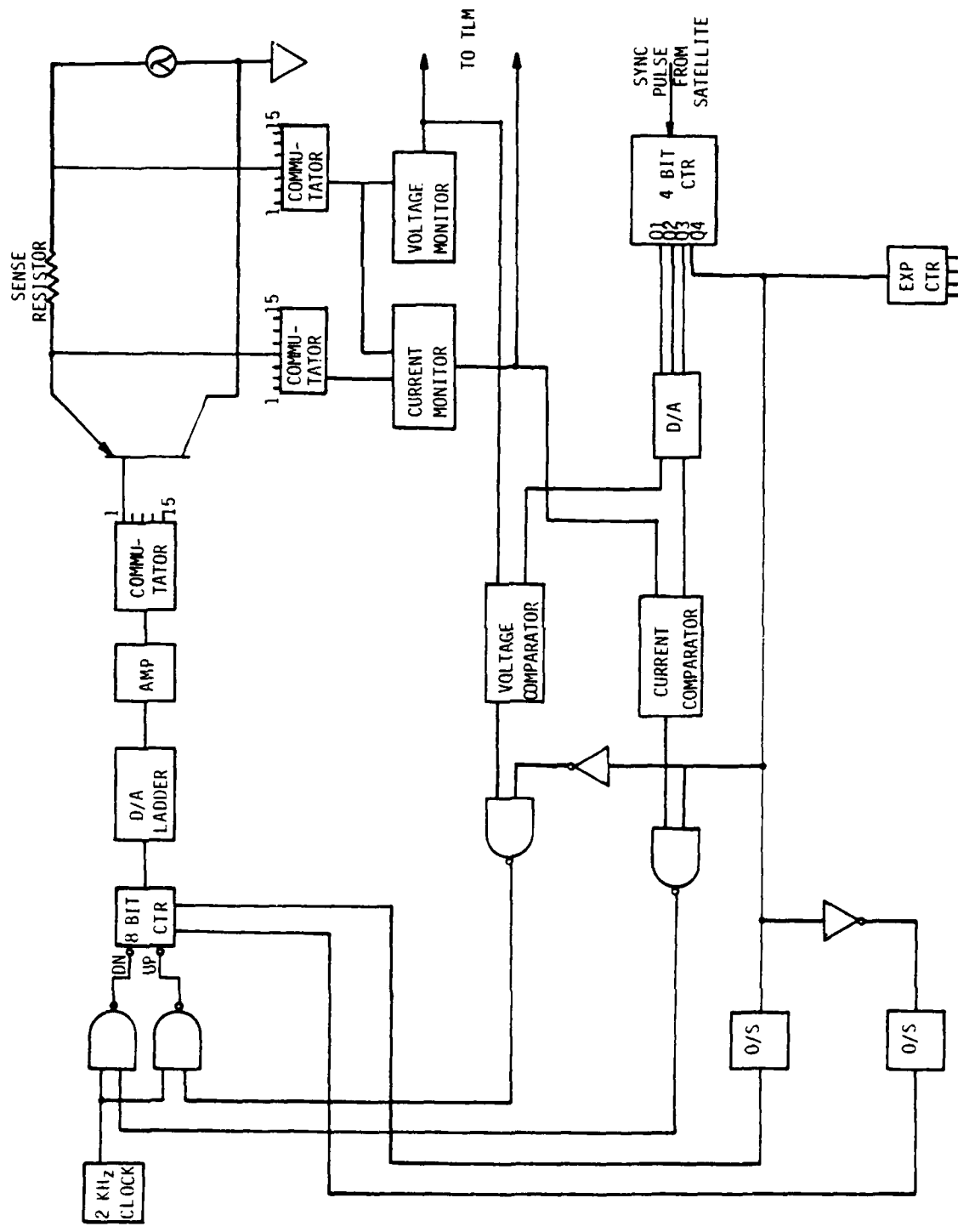


Fig. 2 — The solar cell current-voltage measuring circuit on NTS-2

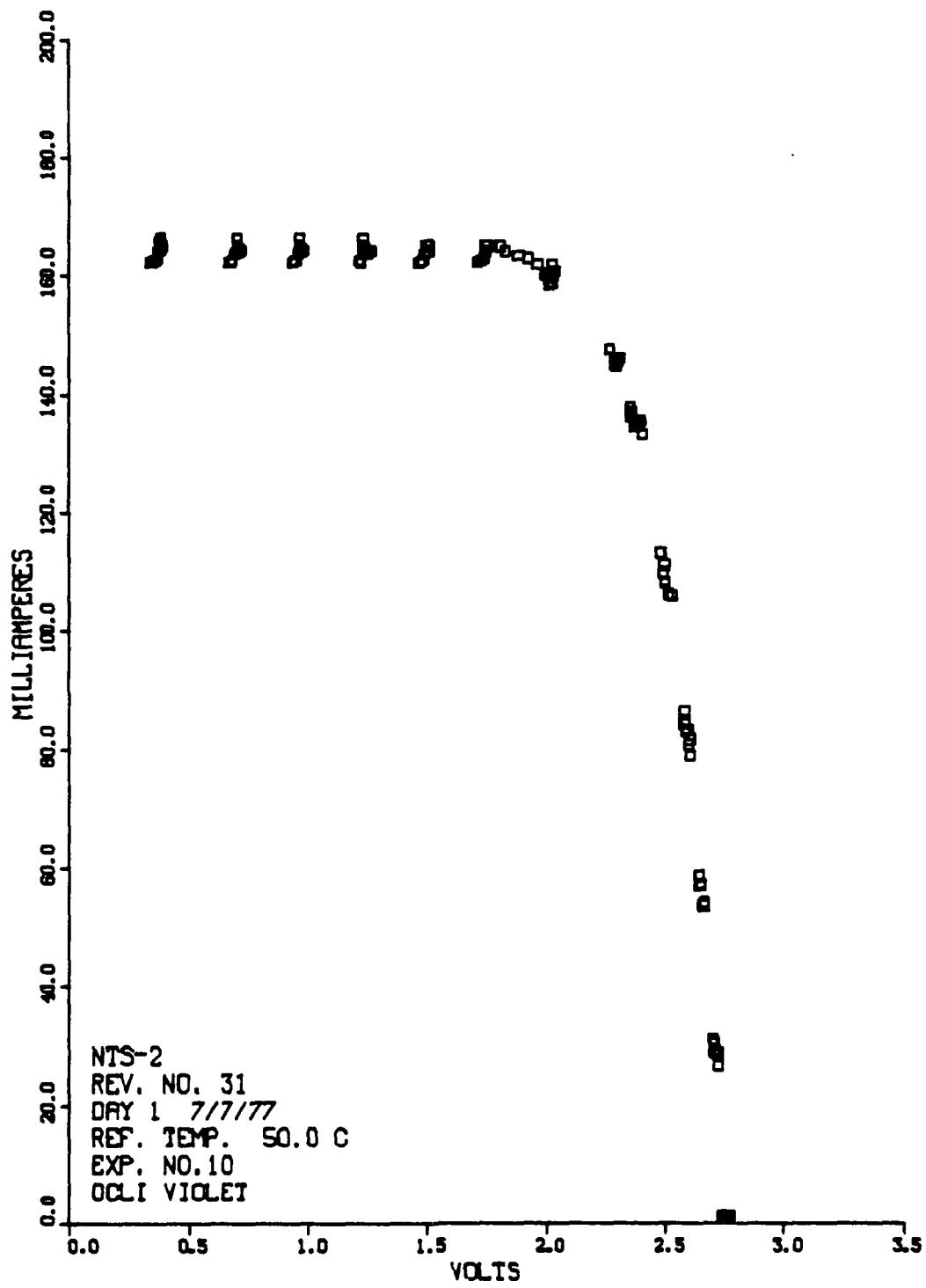


Fig. 3 — A typical current-voltage data curve as received from the NTS-2 satellite, corrected for solar intensity, sun angle and to a temperature of 50°C

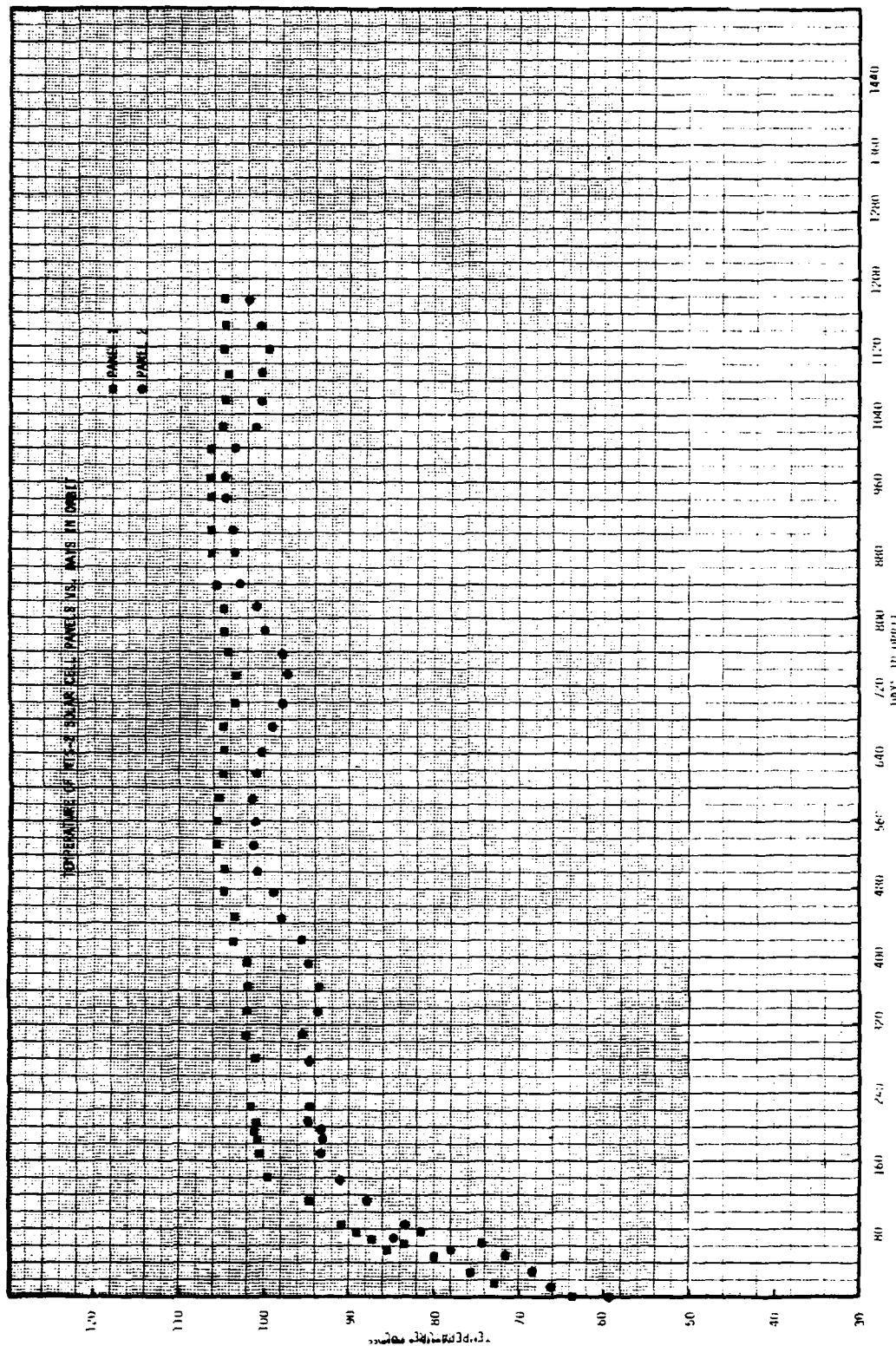


Fig. 4 — The average temperatures of the solar cell panels over the 1,176 days in orbit

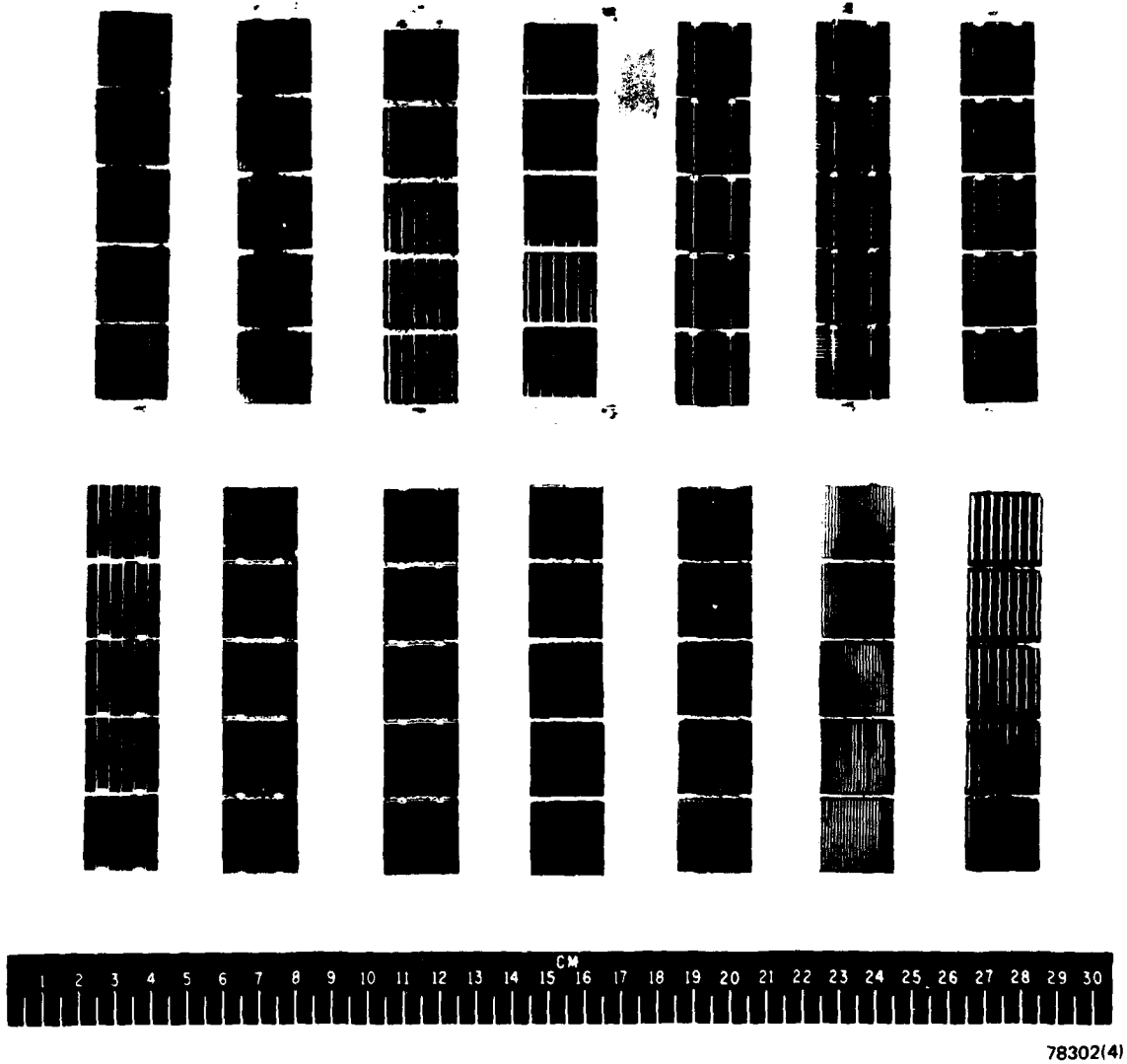


Fig. 5 — The NTS-2 solar cell experiment modules as mounted on the flight panels

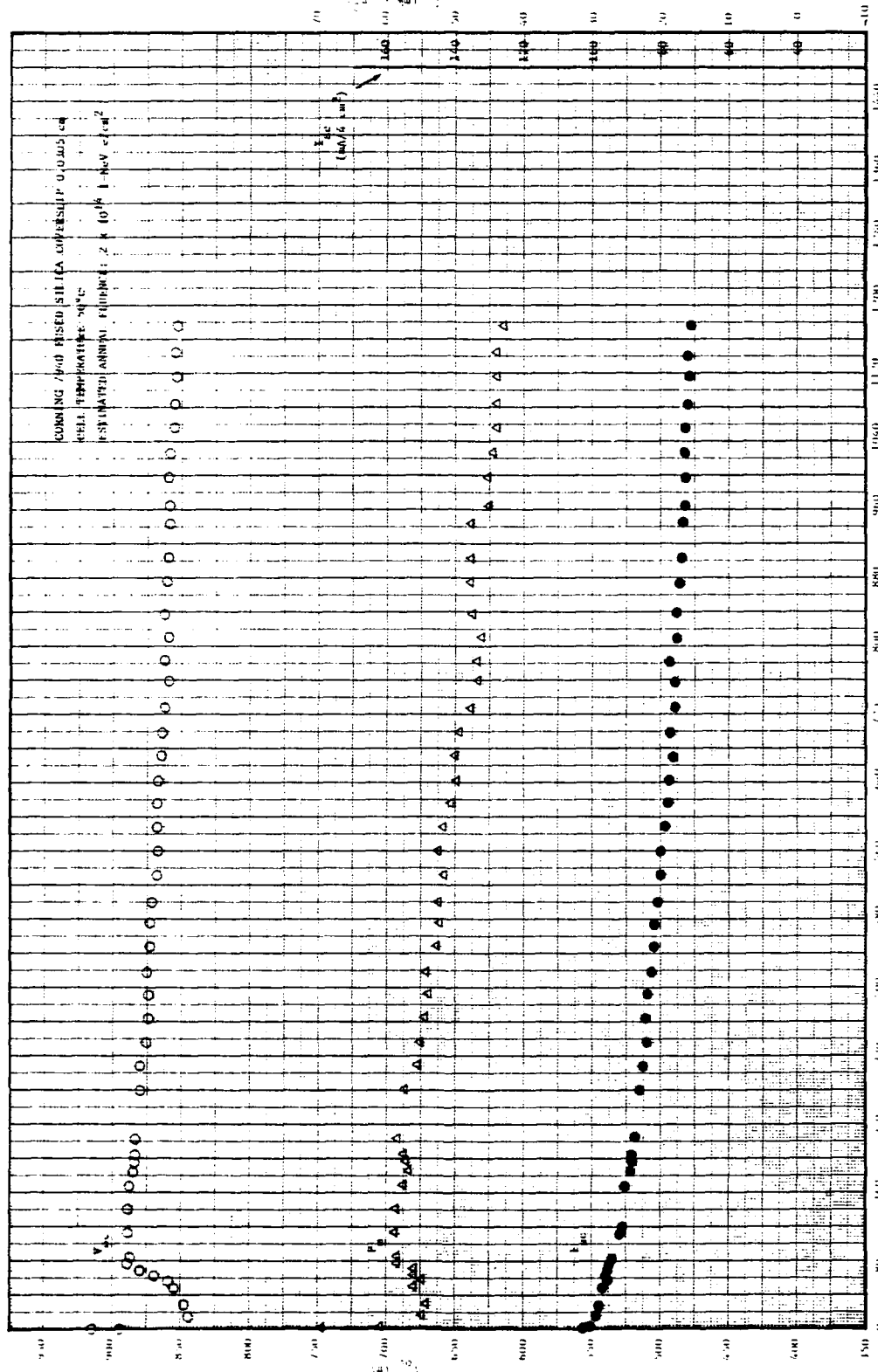


Fig. 6 — Maximum power, short-circuit current, and open-circuit voltage degradation of the Hughes gallium arsenide cell.  $P_{\text{max}}$  and  $I_{\text{sc}}$  are normalized to  $4 \text{ cm}^2$ . (Experiment 15).

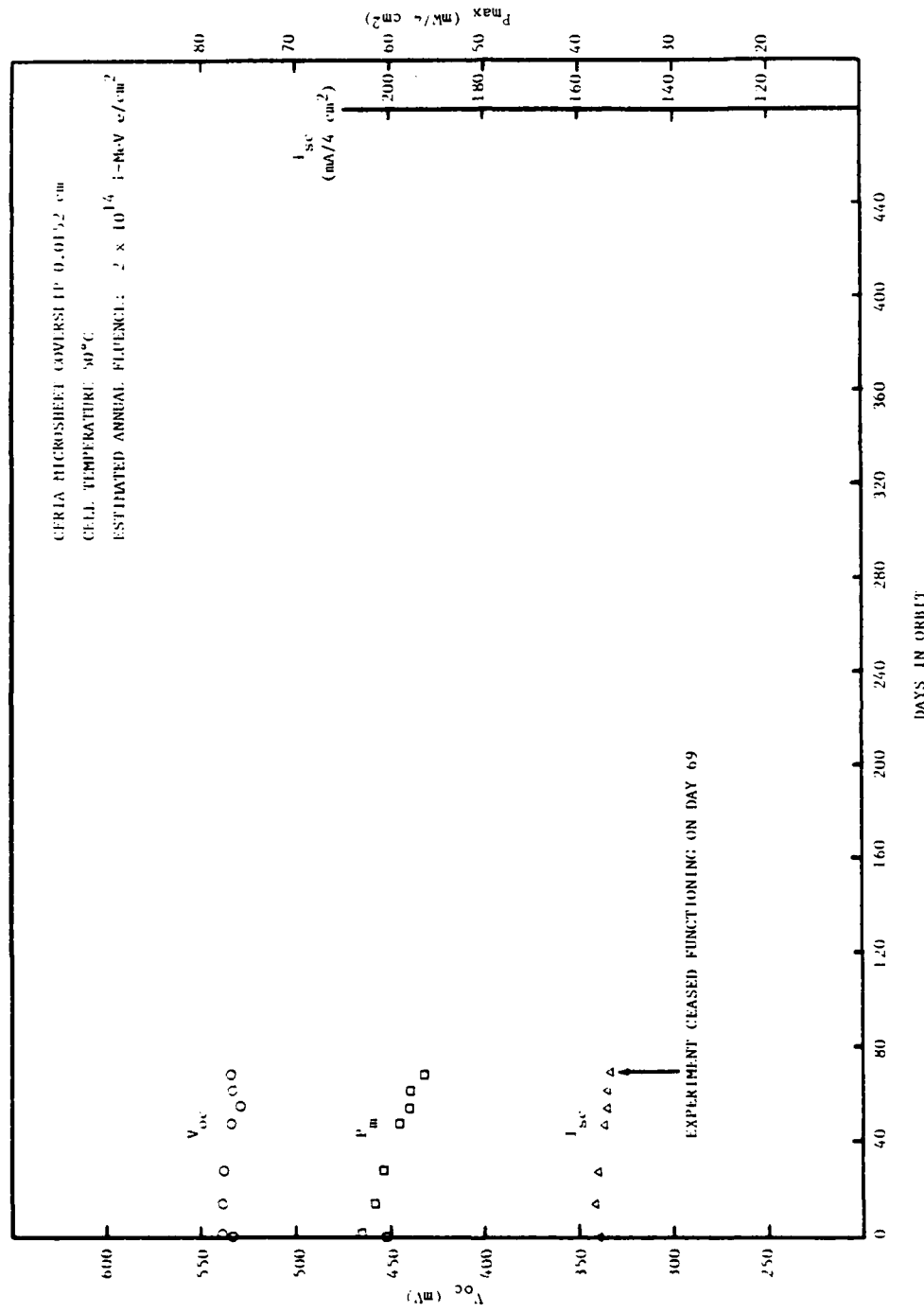
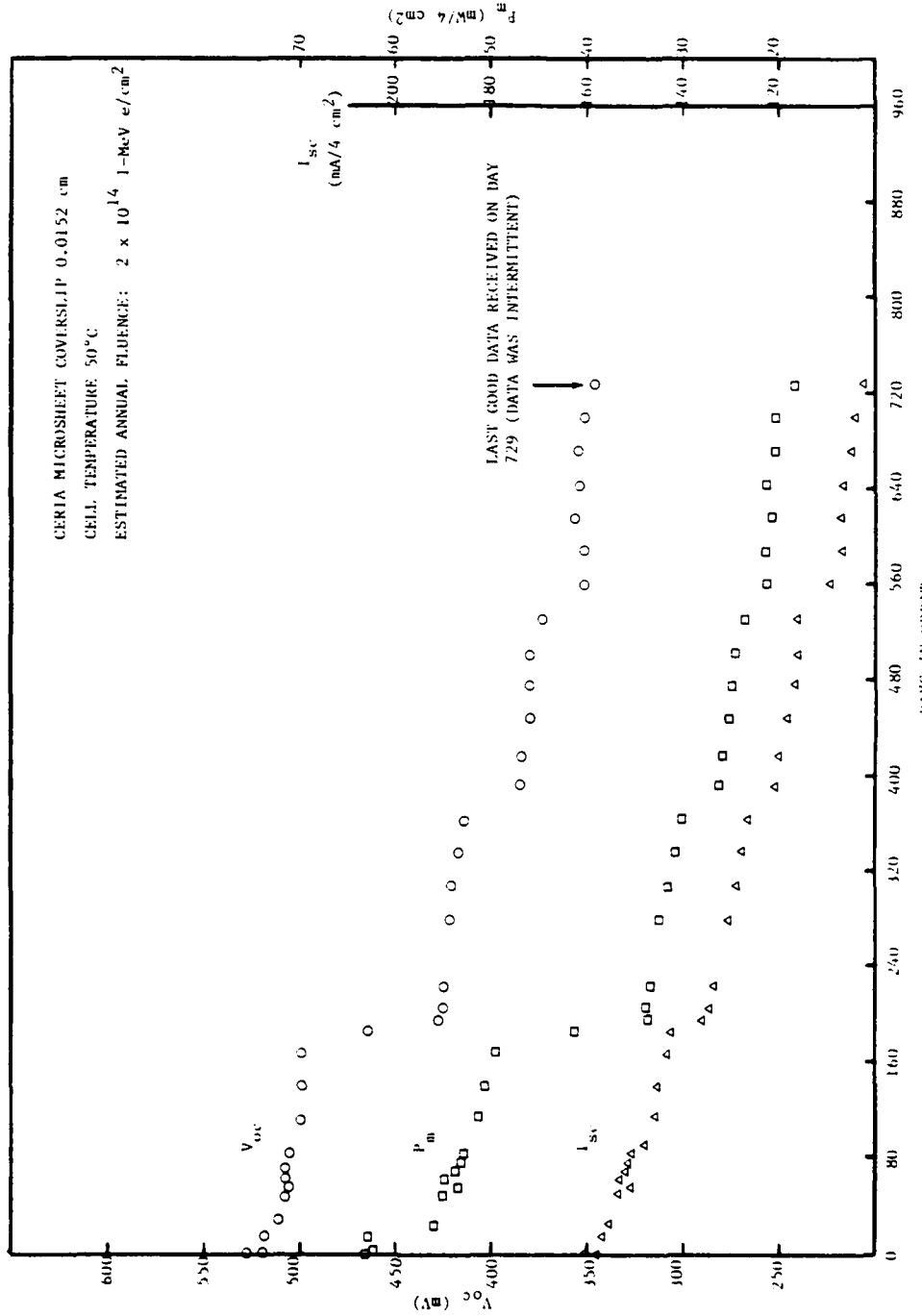


Fig. 7 — Maximum power, short-circuit current, and open-circuit voltage degradation of the Solarex "low-cost space cell."  $P_m$  and  $I_{sc}$  are normalized to 4 cm<sup>2</sup>. (Experiment 8).



**Fig. 8** — Degradation in maximum power, short-circuit current and open-circuit voltage of the Solarex vertical junction solar cell.  $P_m$  and  $I_{sc}$  are normalized to  $4 \text{ cm}^2$ . (Experiment 7).

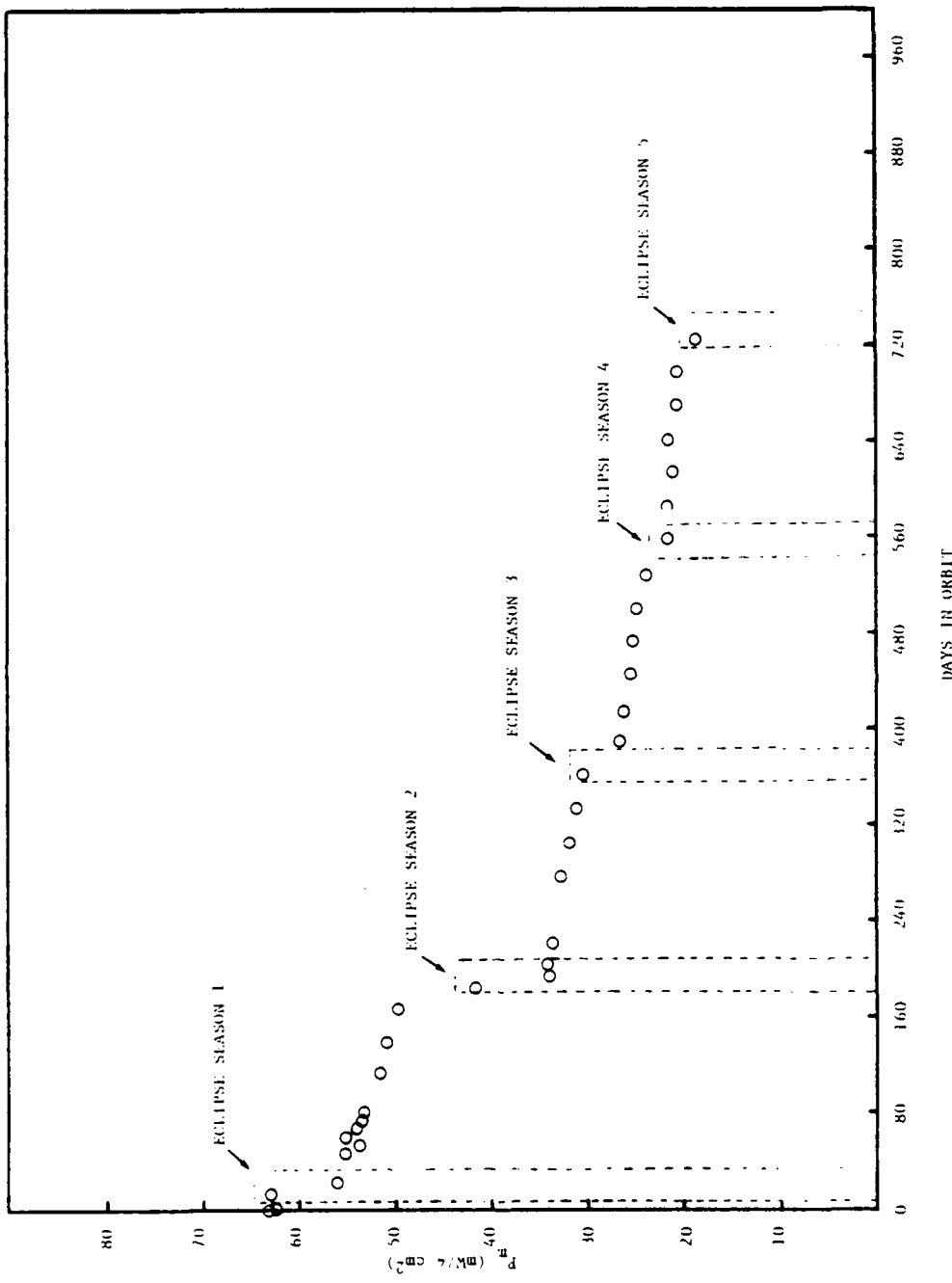


Fig. 9 — Maximum power degradation of the Solarex vertical junction cell relative to the duration of the eclipse versus days in orbit.  $P_m$  is normalized to  $4 \text{ cm}^2$ . Cell temperature is  $50^\circ\text{C}$ .

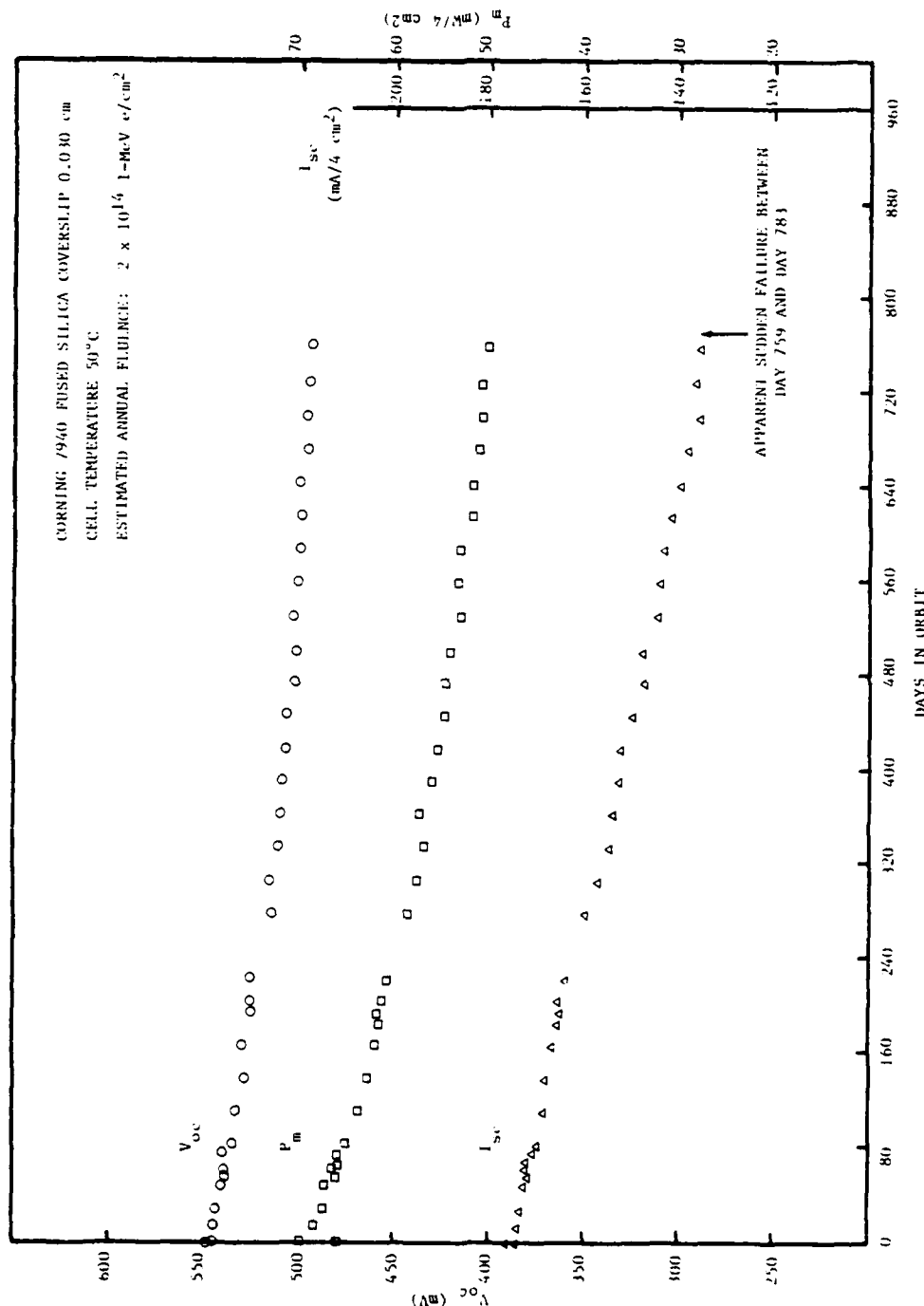


Fig. 10 — Degradation of  $P_m$ ,  $V_{oc}$  and  $I_{sc}$  of the Spectrolab Helios reflector cells.  
 $P_m$  and  $I_{sc}$  are normalized to 4 cm<sup>2</sup>. (Experiment 9).

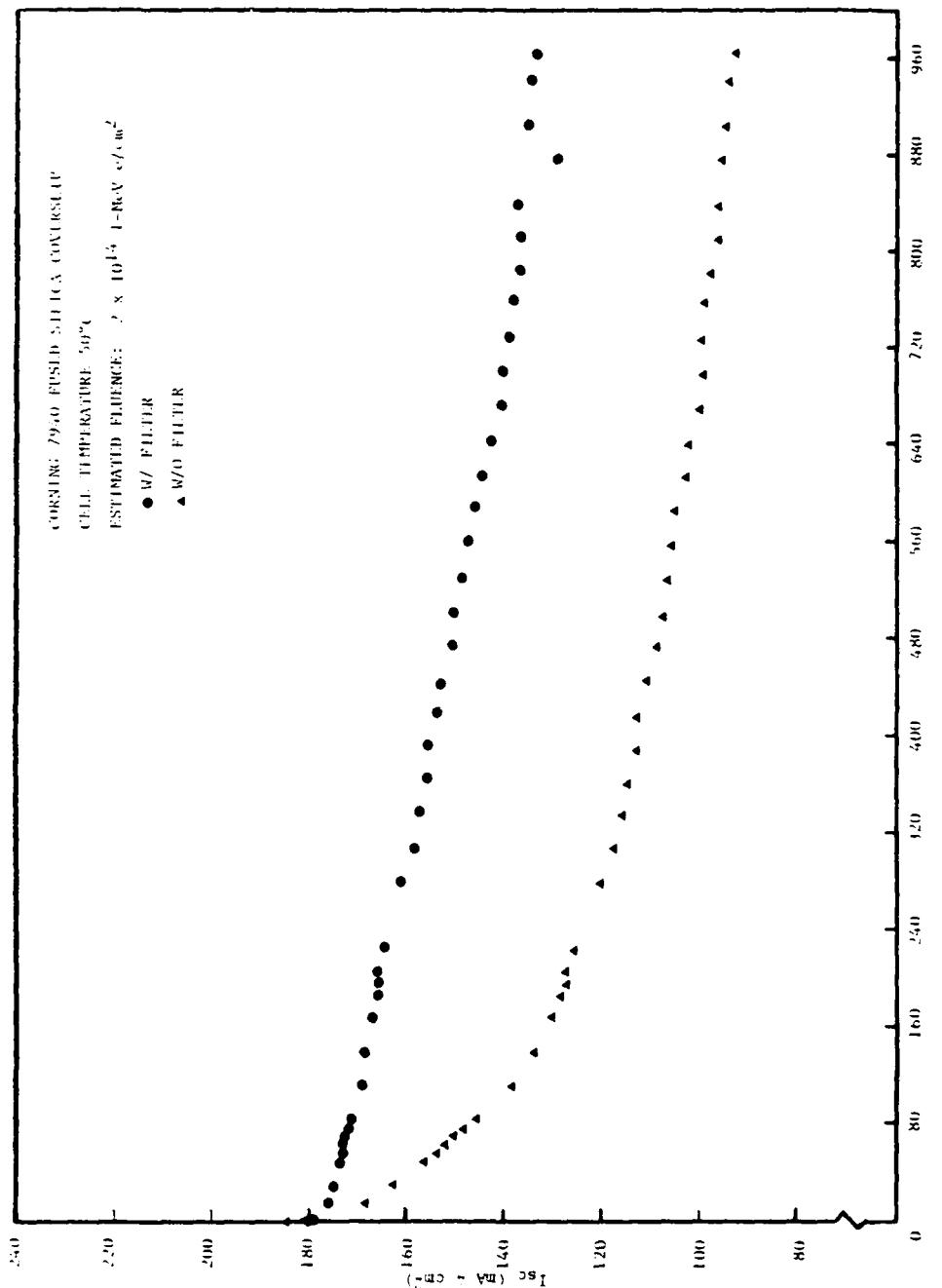


Fig. 11 — Comparison of the short-circuit current degradation of the Comsat textured cells with and without an ultraviolet rejection filter

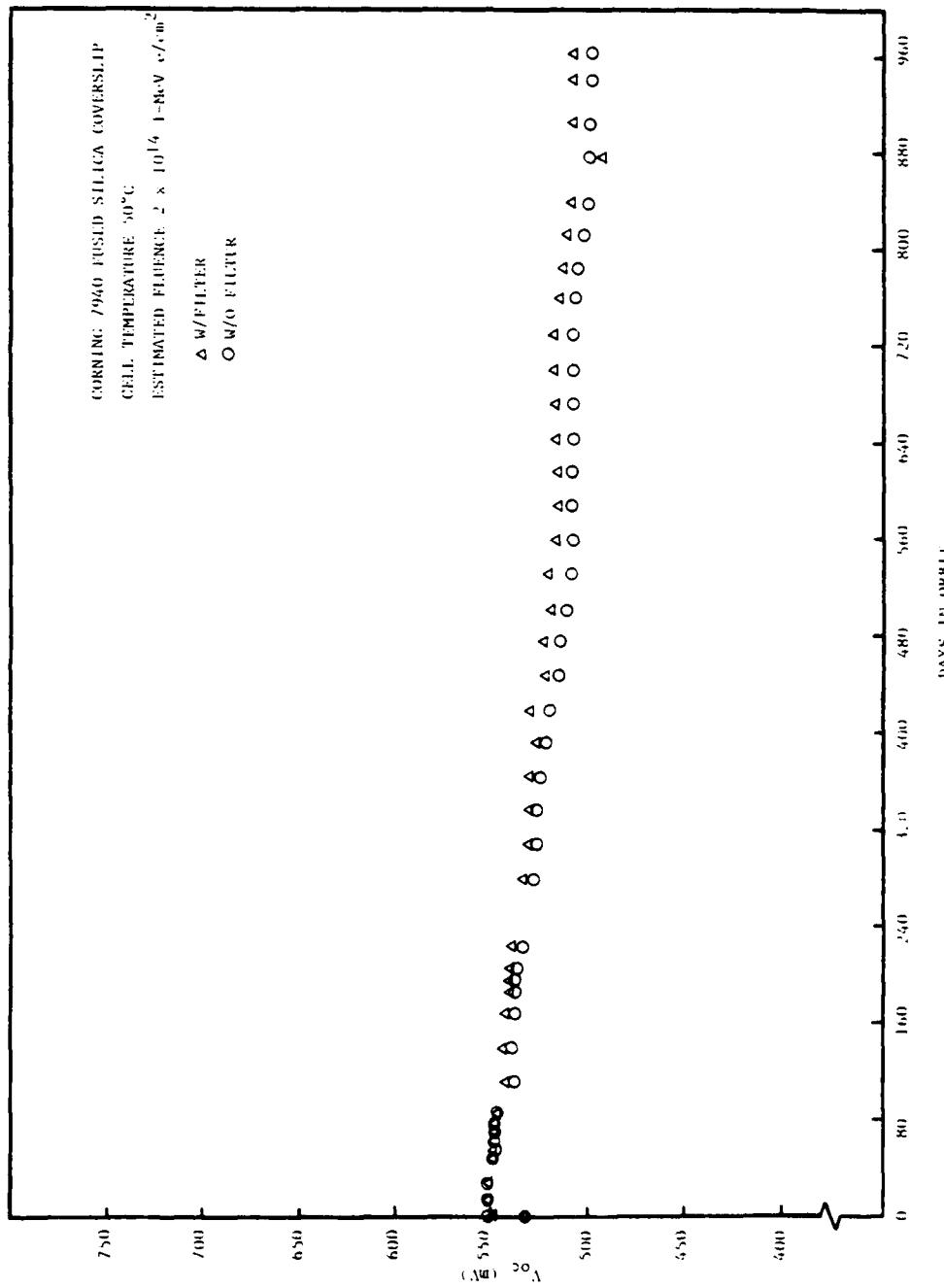


Fig. 12 — Comparison of the open-circuit voltage degradation of the Comsat textured cells with and without an ultraviolet rejection filter

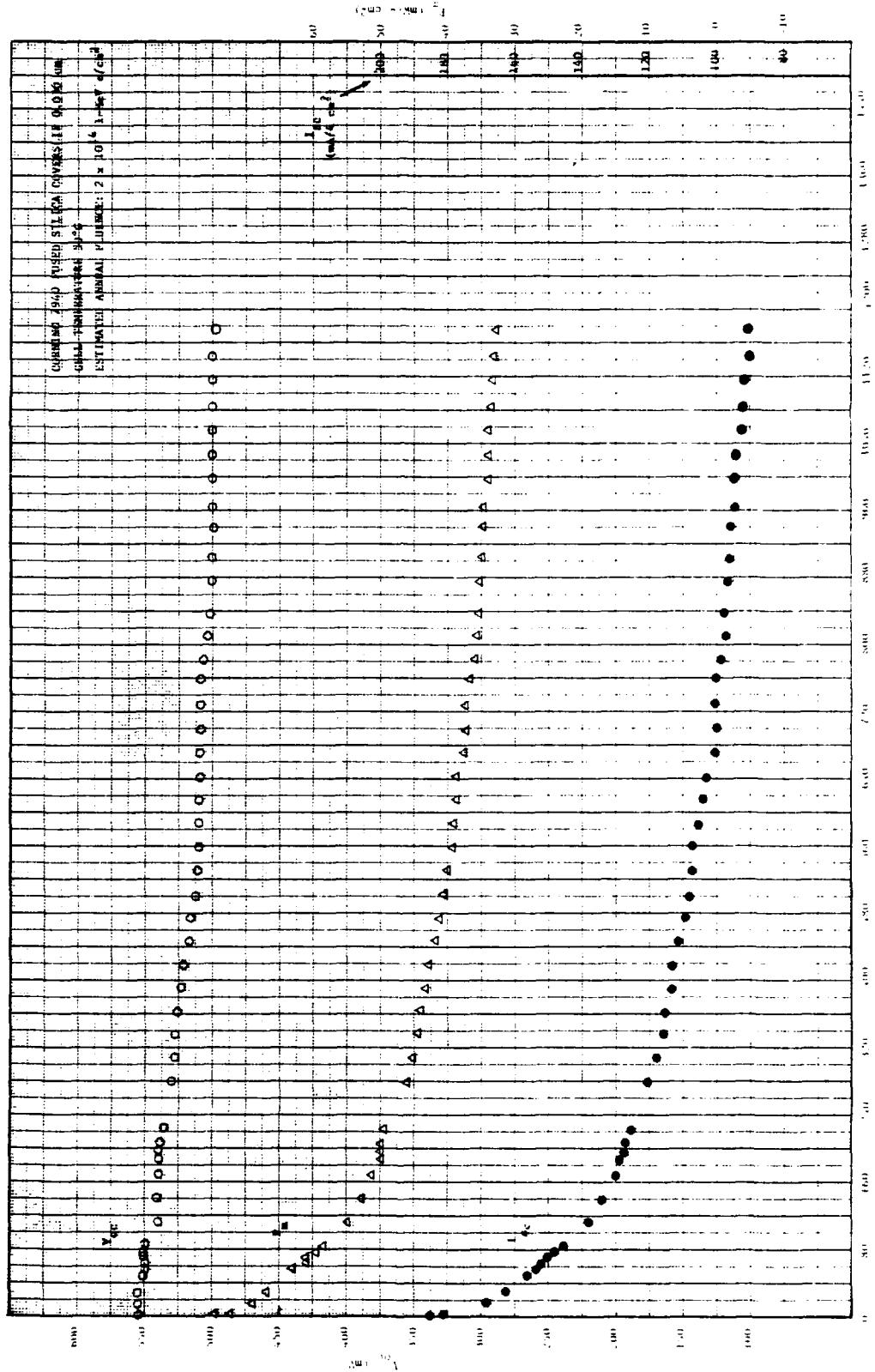


Fig. 13 — Degradation of maximum power, short-circuit current and open-circuit voltage of the Comsat CNR cell without the ultraviolet filter. (Experiment 5).

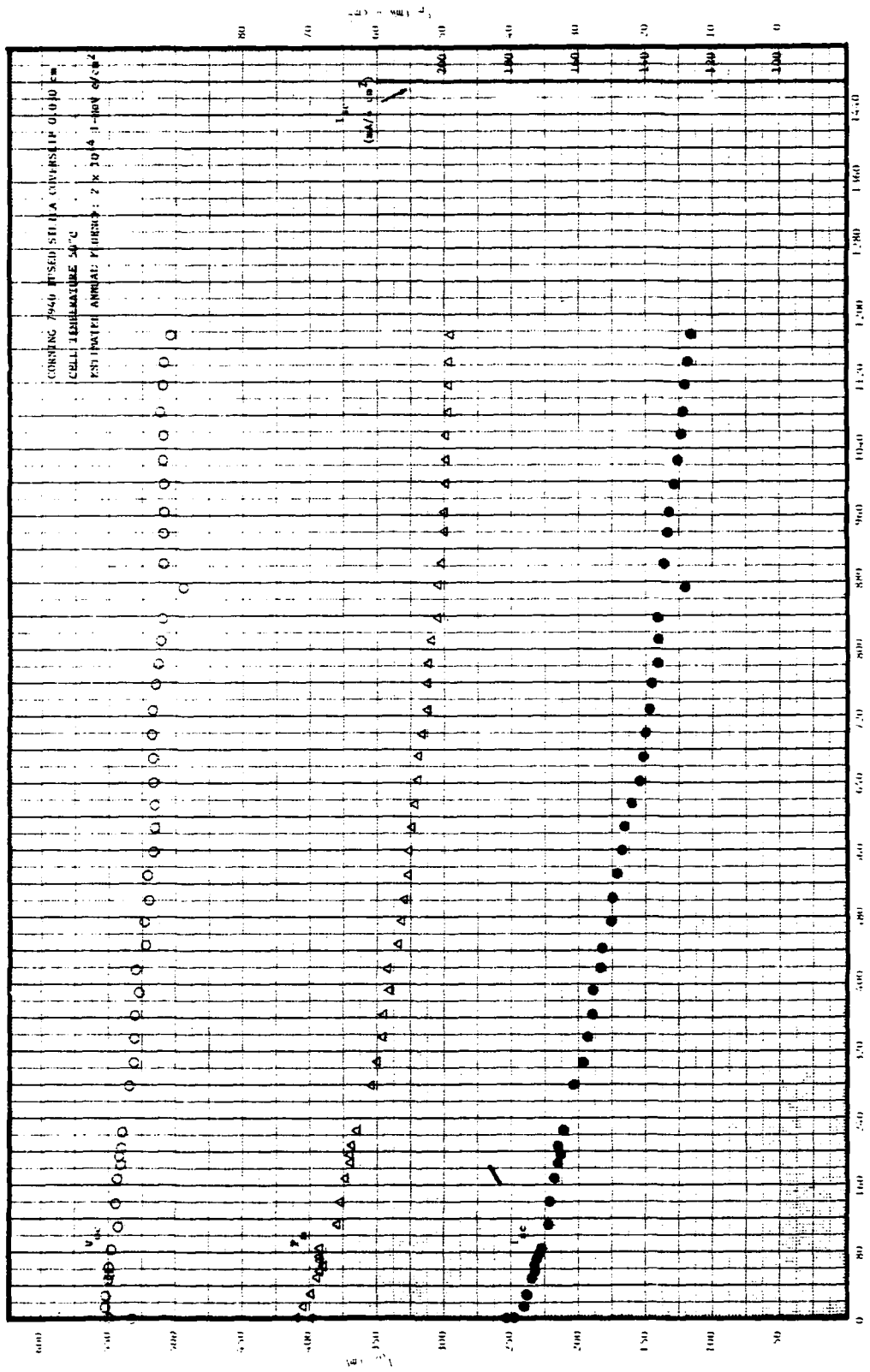


Fig. 14 — Degradation of maximum power, short-circuit current and open-circuit voltage of the Comsat CNR cell with an ultraviolet rejection filter. (Experiment 6).

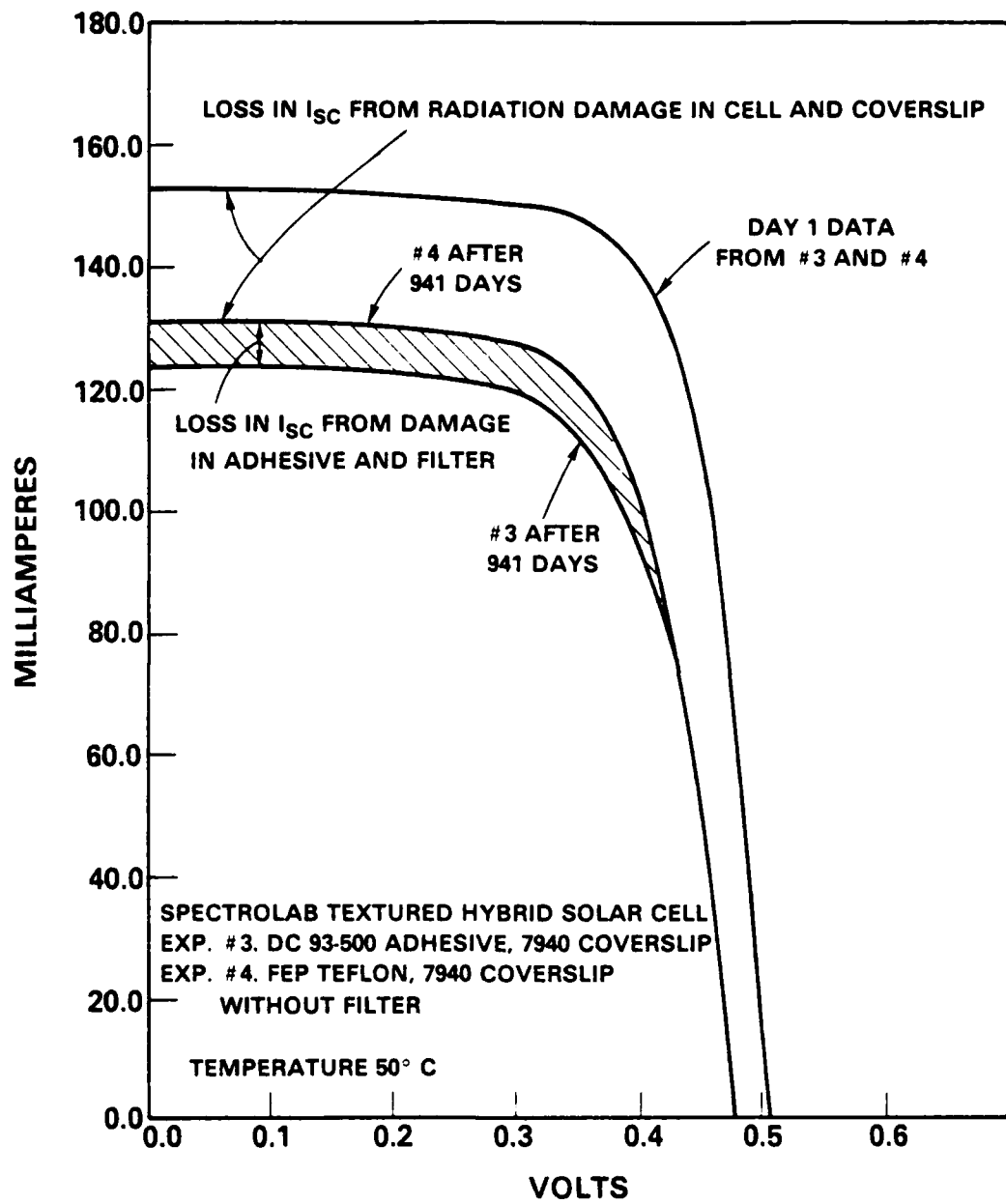


Fig. 15 — I-V curves from the first day in orbit and after 941 days of Spectrolab textured hybrid cells with and without an ultraviolet rejection filter and with both adhesive and FEP Teflon bonded coverslips

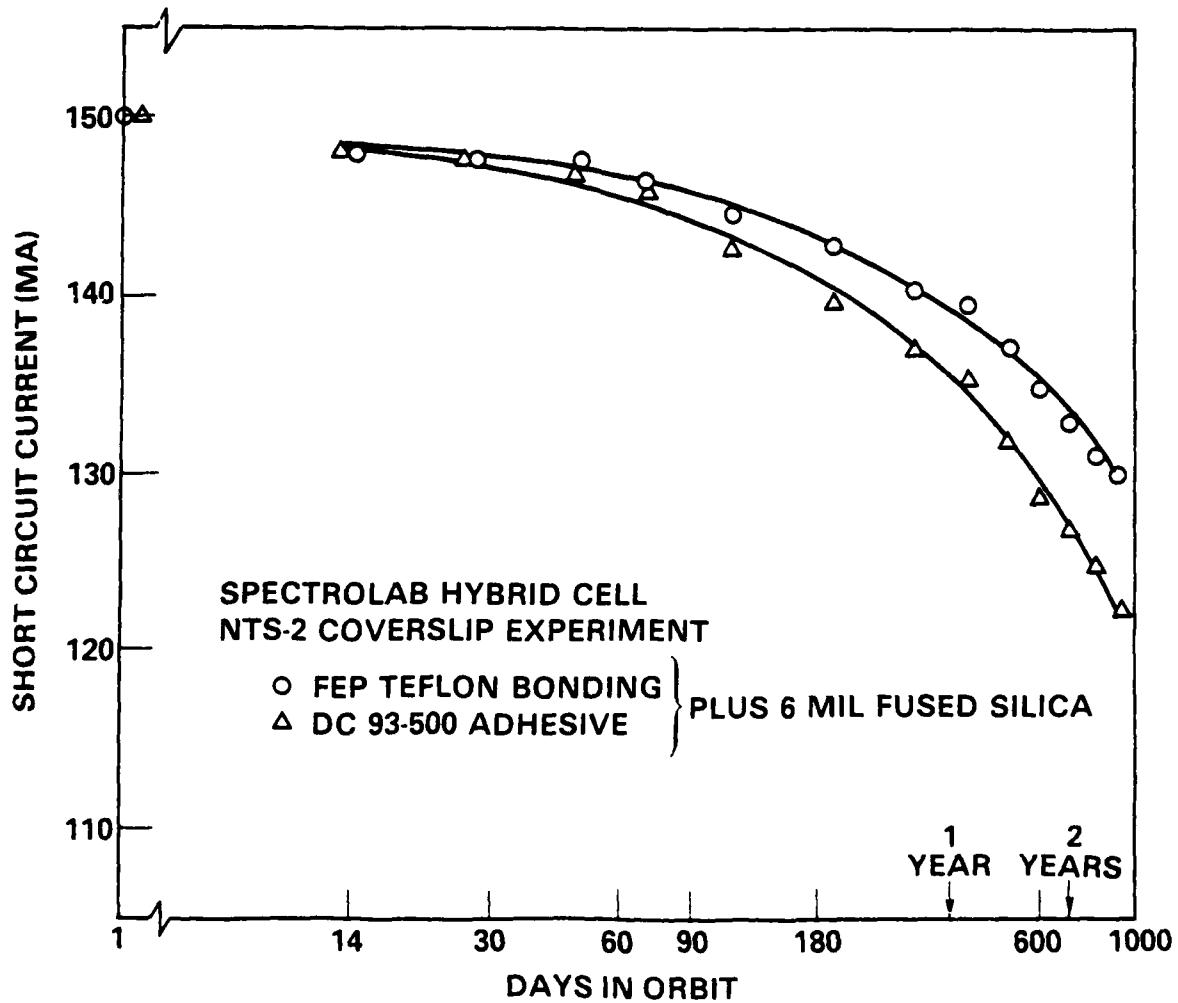


Fig. 16 — Comparison of the short-circuit current degradation of the Spectrolab textured hybrid cells with adhesively bonded coverslips and with FEP Teflon bonded coverslips. Cell temperature is 50°C.

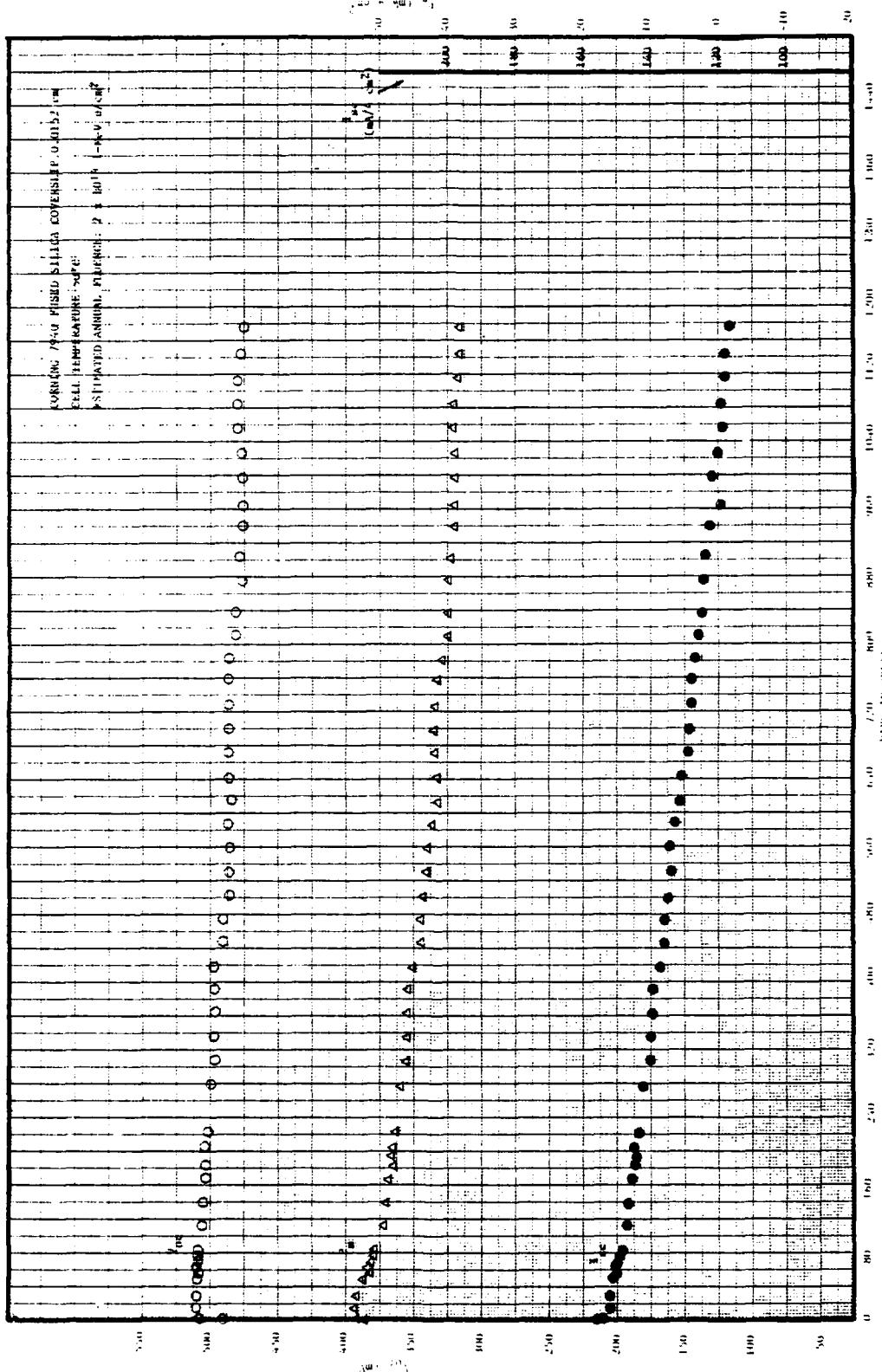


Fig. 17 — Degradation of  $P_m$ ,  $I_{sc}$  and  $V_{oc}$  of the Spectrolab textured hybrid cell.  
 $P_m$  and  $I_{sc}$  are normalized to 4 cm<sup>2</sup>. (Experiment 3).

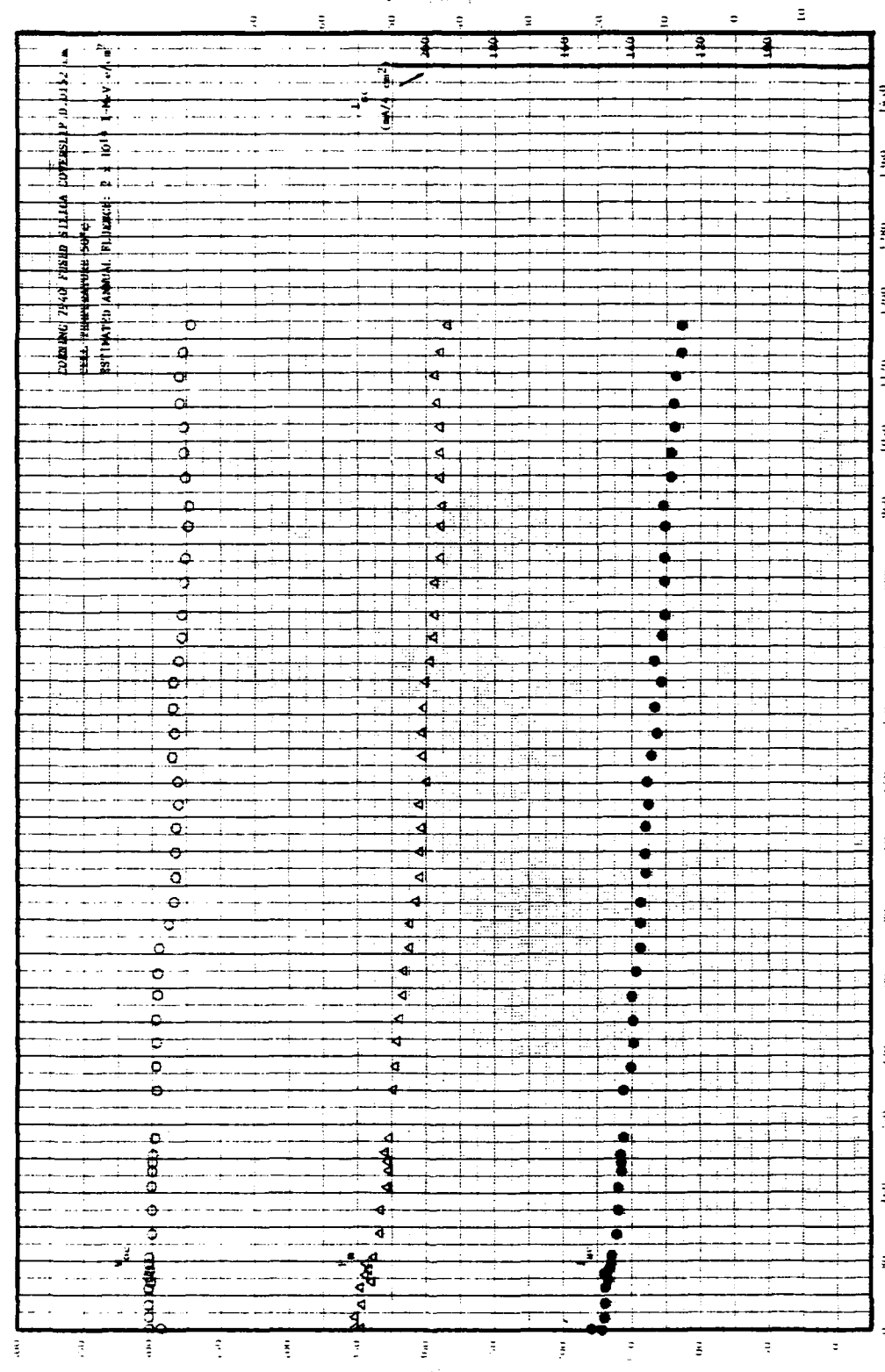


Fig. 18 — Degradation of  $P_m$ ,  $I_m$  and  $V_{oc}$  of the Spectrolab textured hybrid solar cell with FEP Teflon bonded coverslip.  $P_m$  and  $I_m$  are normalized to  $4 \text{ cm}^2$ . (Experiment 4).

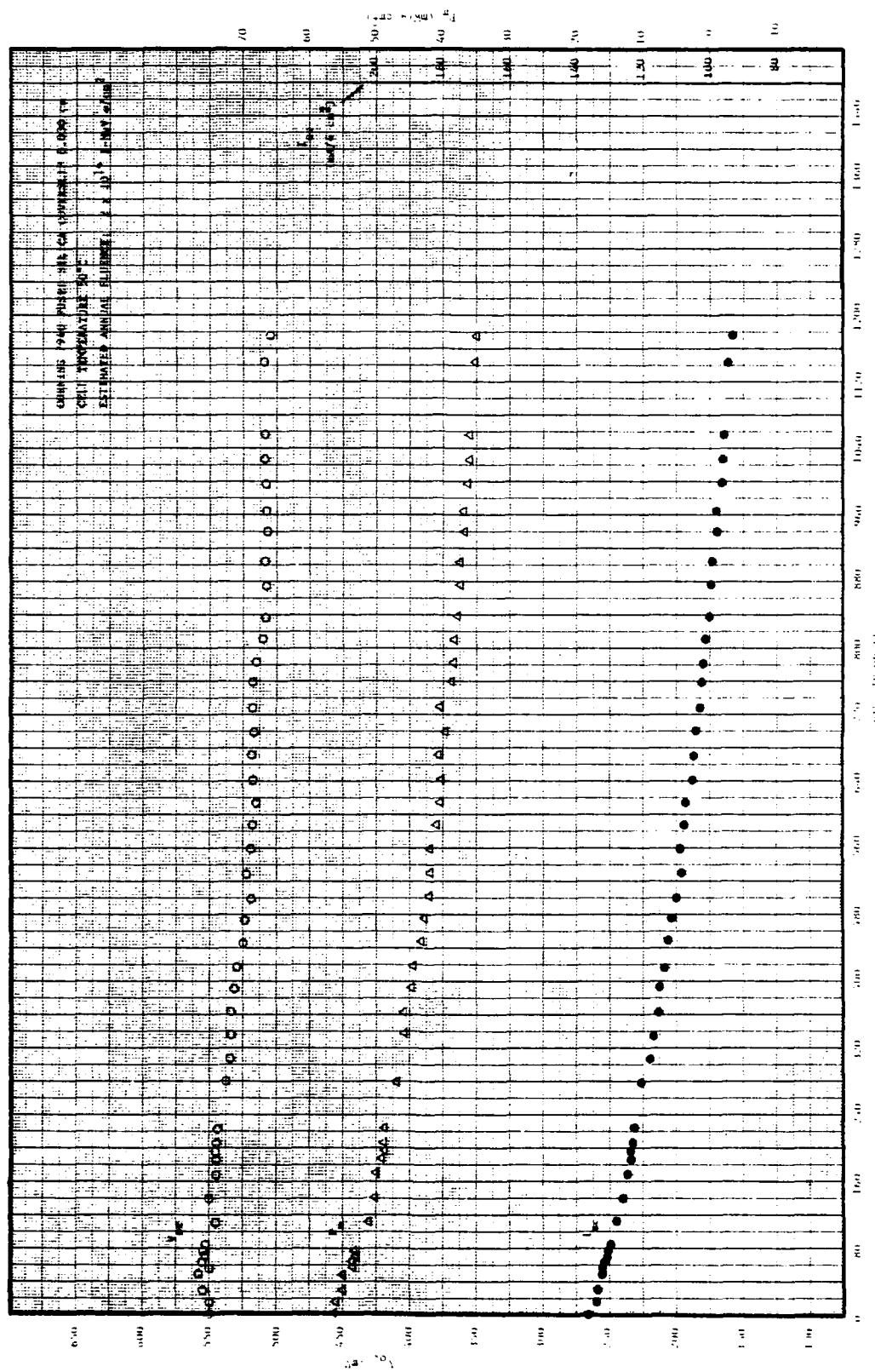


Fig. 19 – Degradation of maximum power, short-circuit current and open-circuit voltage of the OCLJ conventional solar cell.  $P_m$  and  $I_{sc}$  are normalized to  $4 \text{ cm}^2$ . (Experiment 1).

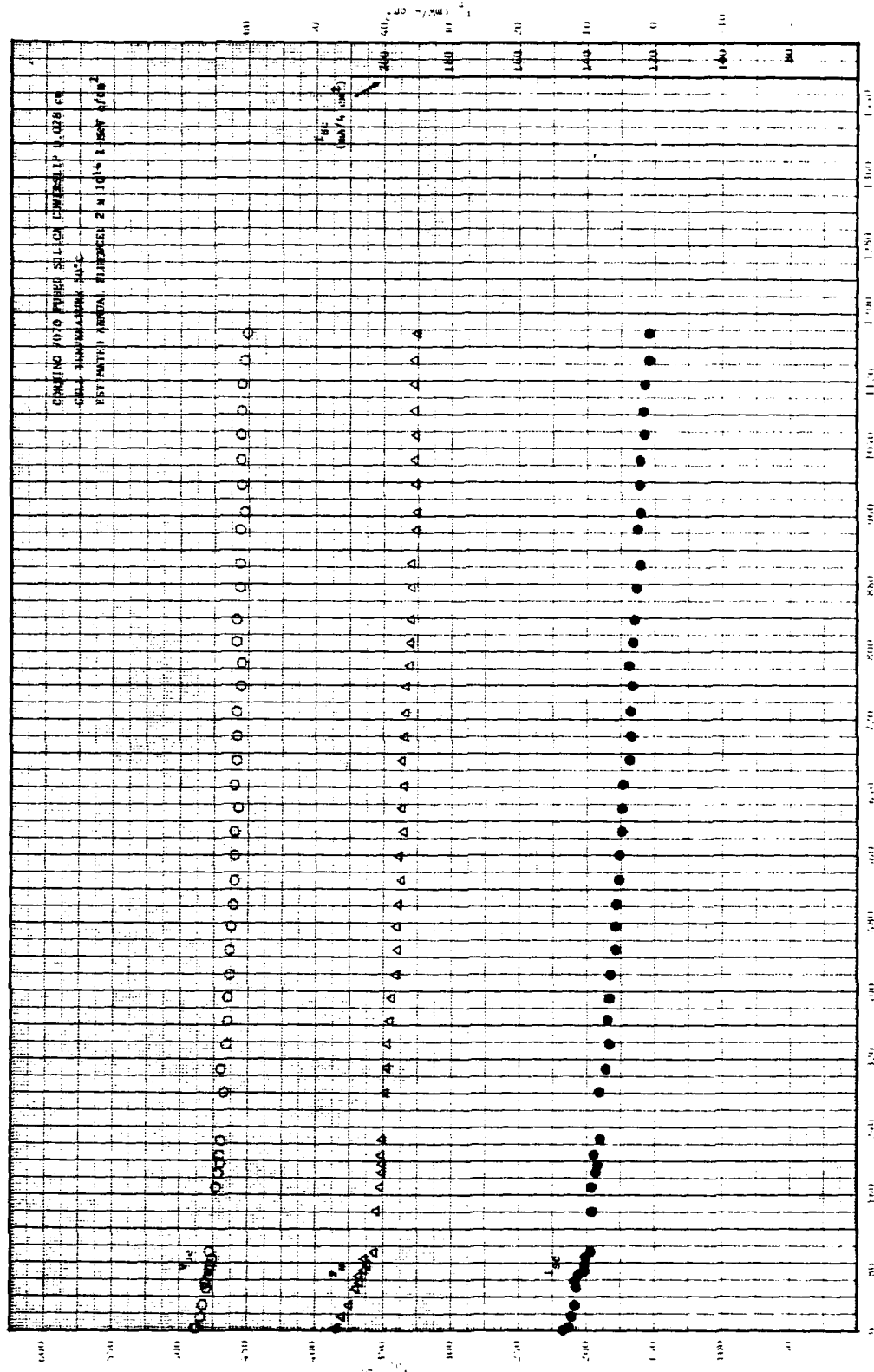


Fig. 20 — Degradation of  $P_m$ ,  $I_{sc}$  and  $V_{oc}$  of the OCLJ conventional solar cell with electrostatically bonded coverslip.  $P_m$  and  $I_{sc}$  are normalized to 4 cm<sup>2</sup>. (Experiment 13).

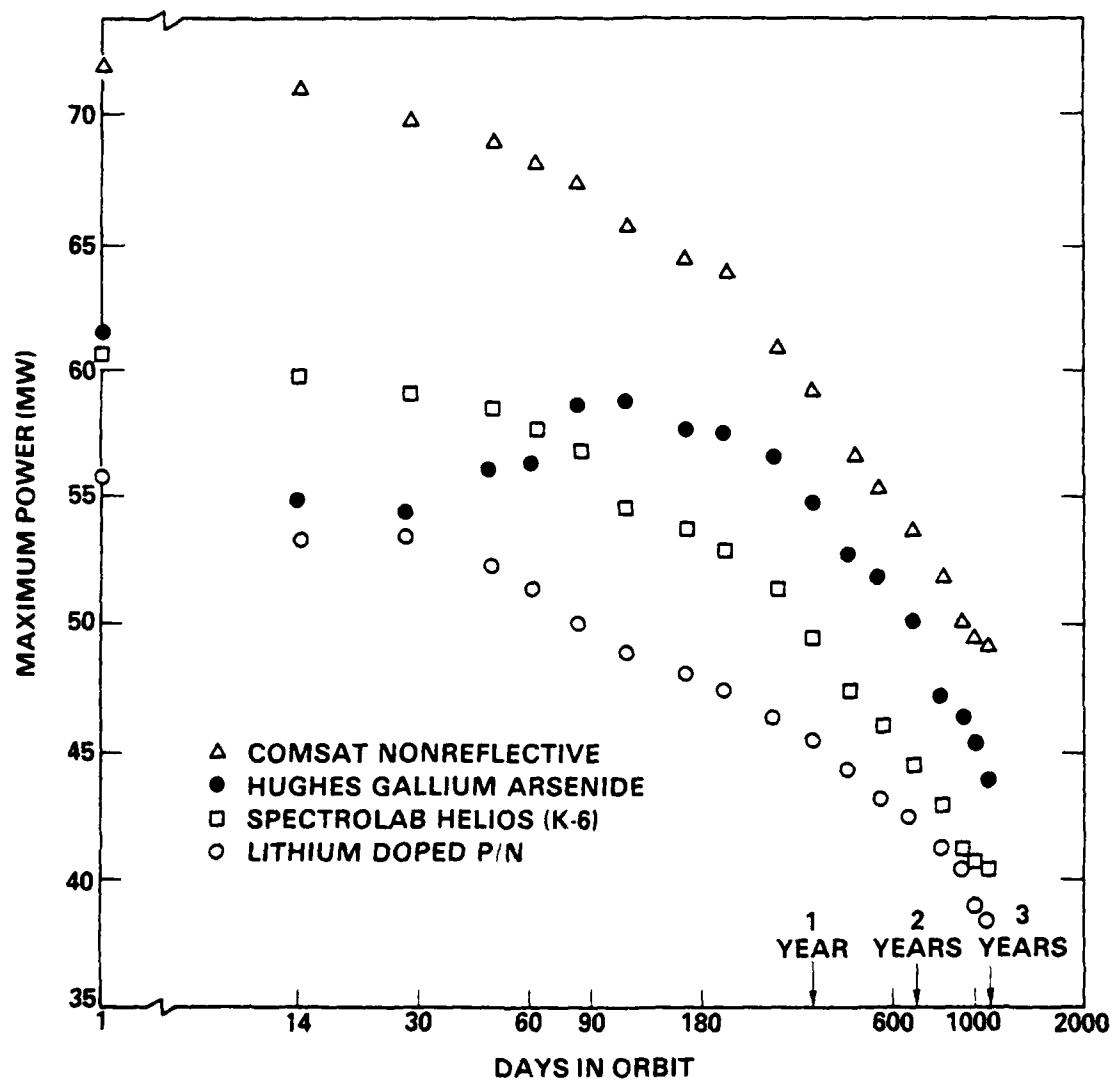


Fig. 21 — Comparison of the power degradation of the Comsat nonreflective, Hughes gallium arsenide, Spectrolab Helios (K-6) and the lithium-doped p/n solar cells. Cell temperature is 50°C.

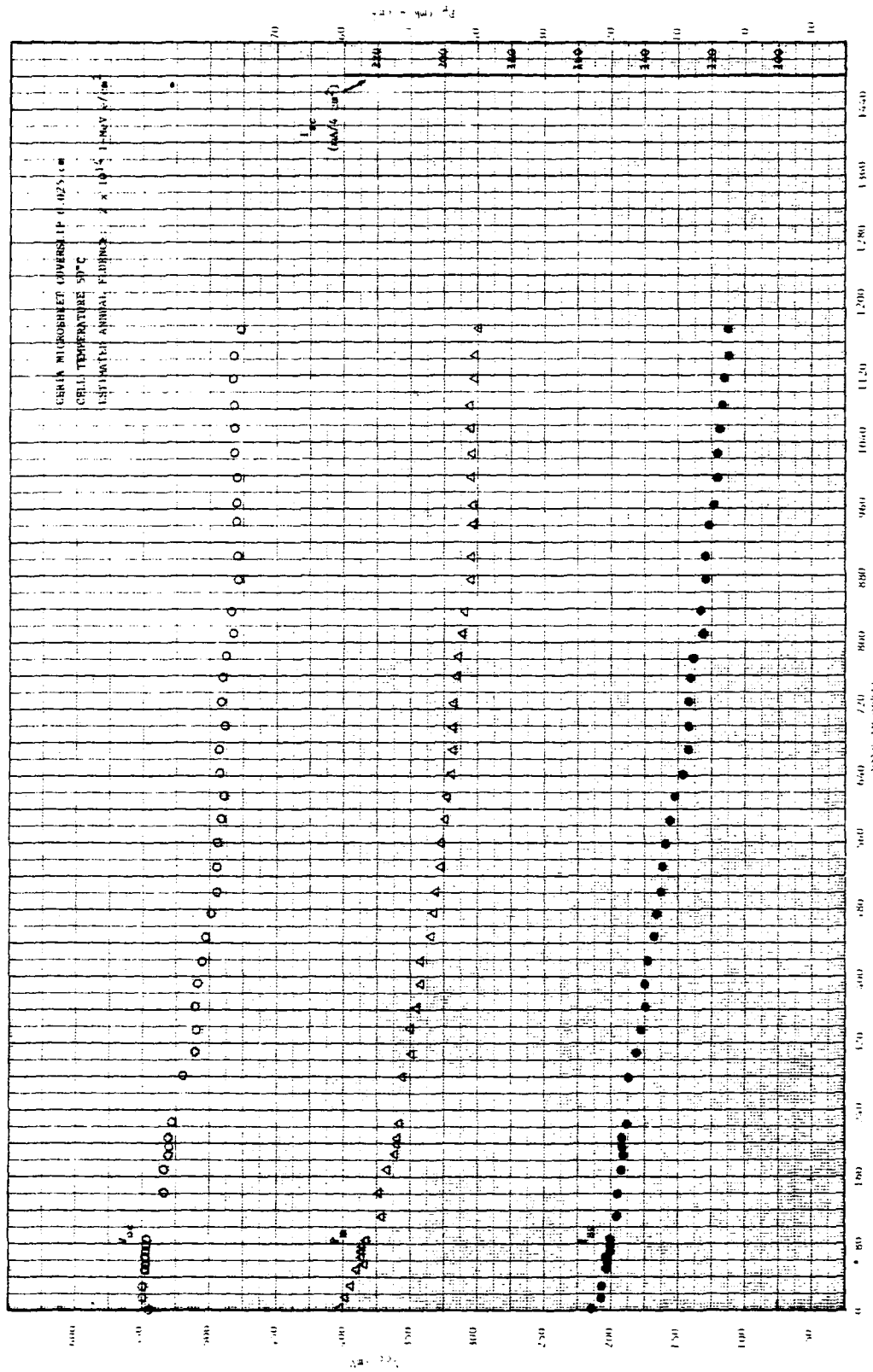


Fig. 22 — Degradation of  $P_m$ ,  $I_{sc}$  and  $V_{oc}$  of the Spectrolab Helios cell.  
 $P_m$  and  $I_{sc}$  are normalized to  $4 \text{ cm}^2$ . (Experiment 2).

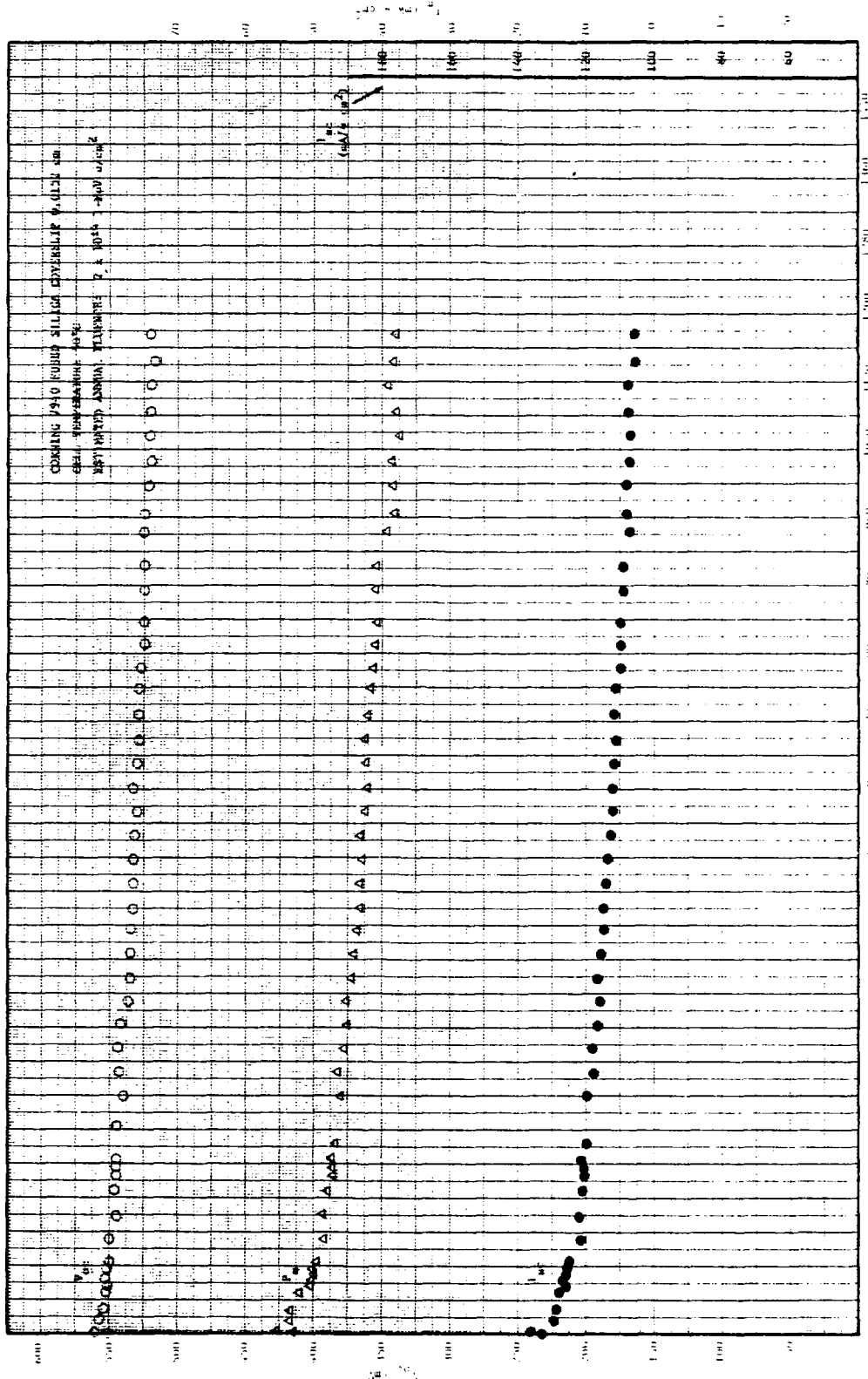


Fig. 23 — Degradation of  $P_m$ ,  $I_{sc}$  and  $V_{oc}$  of the Spectrolab HASP cell (lithium-doped). (Experiment 11).

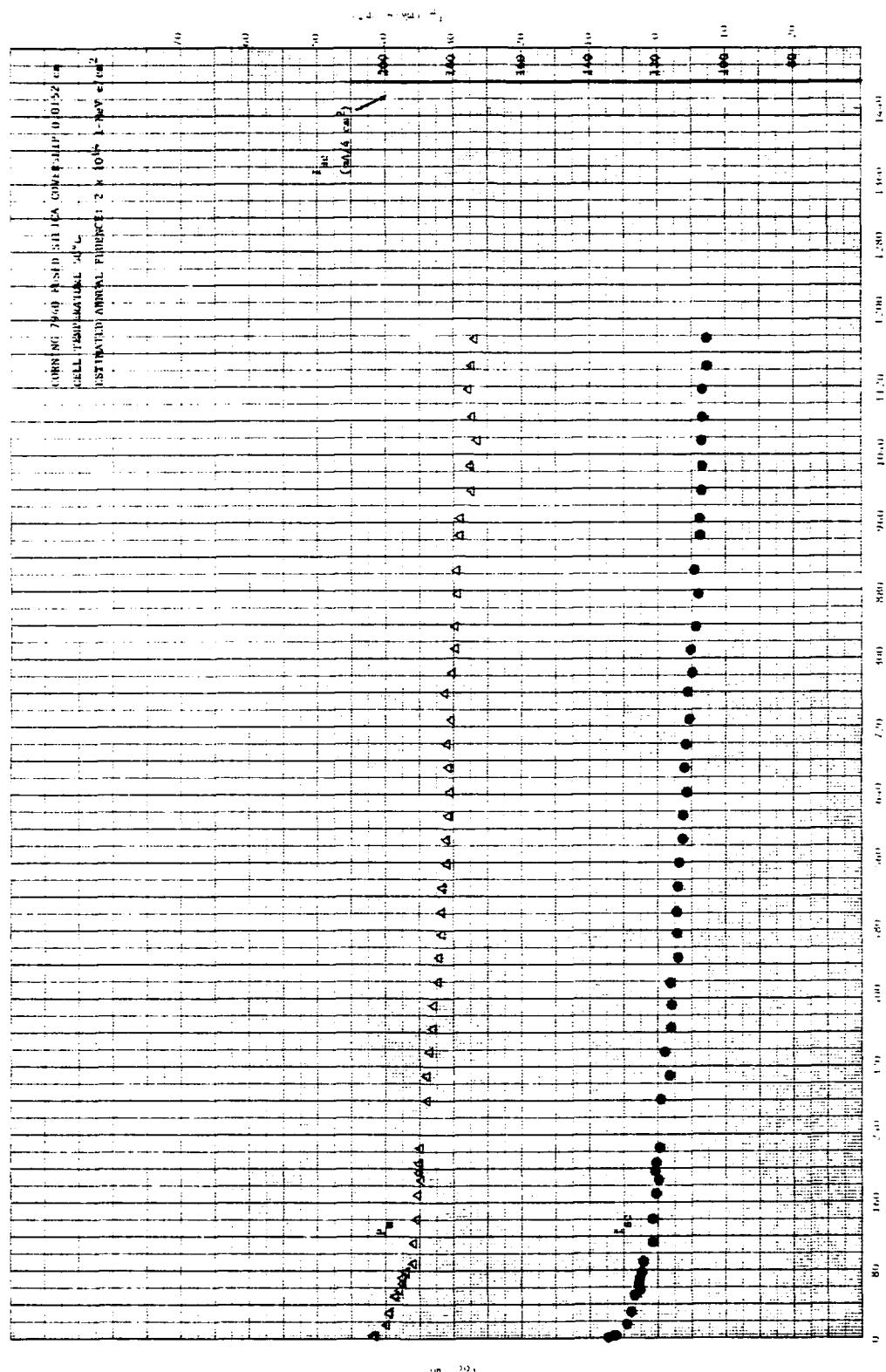


Fig. 24 — Degradation of  $P_m$ ,  $I_{sc}$  and  $V_{oc}$  of the Spectrolab lithium-doped IASp solar cell in series with a planar diode. (Experiment 12).

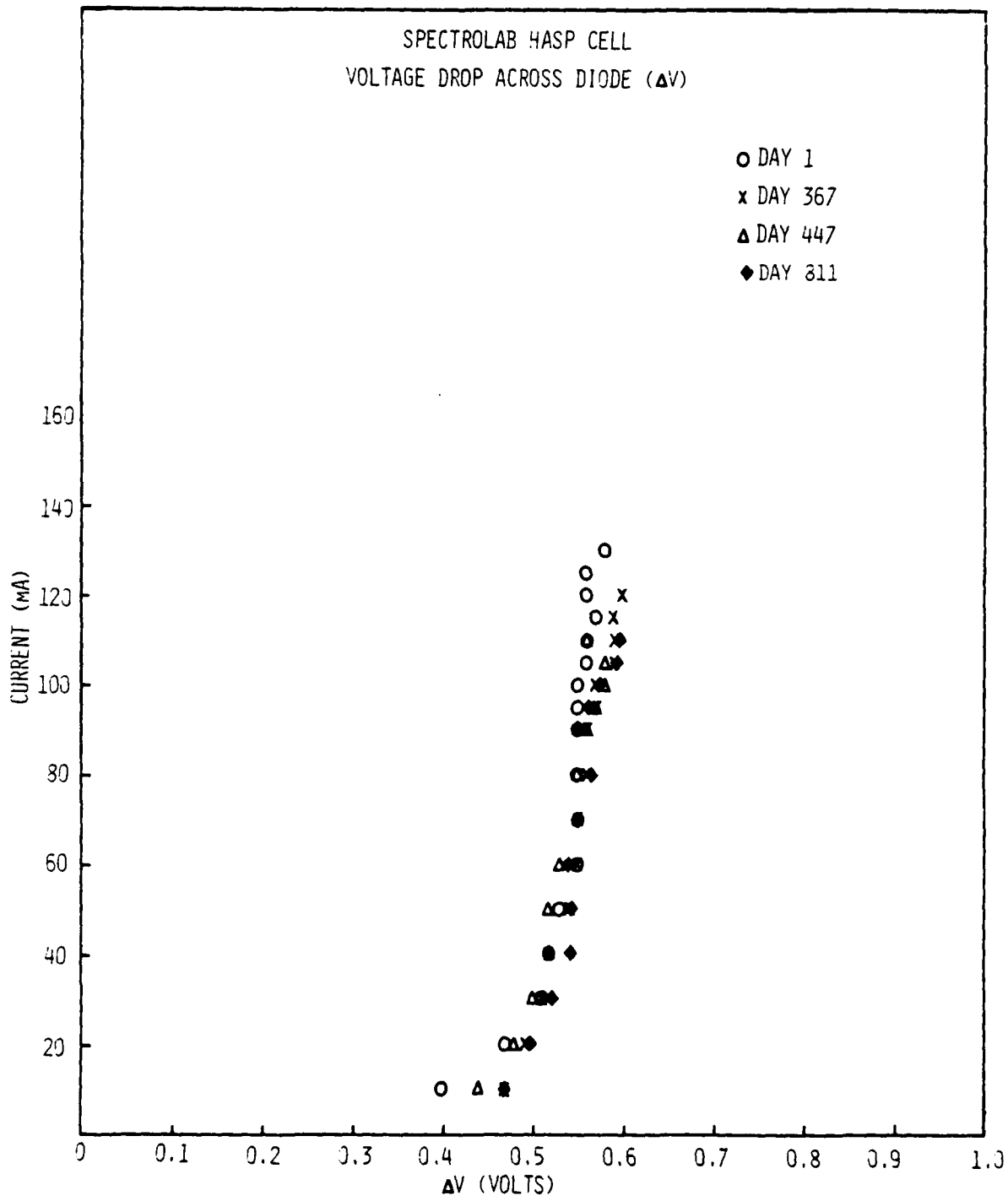


Fig. 25 — Comparison of the changes in voltage drop across the diode in series with the Spectrolab lithium-doped HASP solar cell from day 1 through day 811. Cell temperature is 50° C.

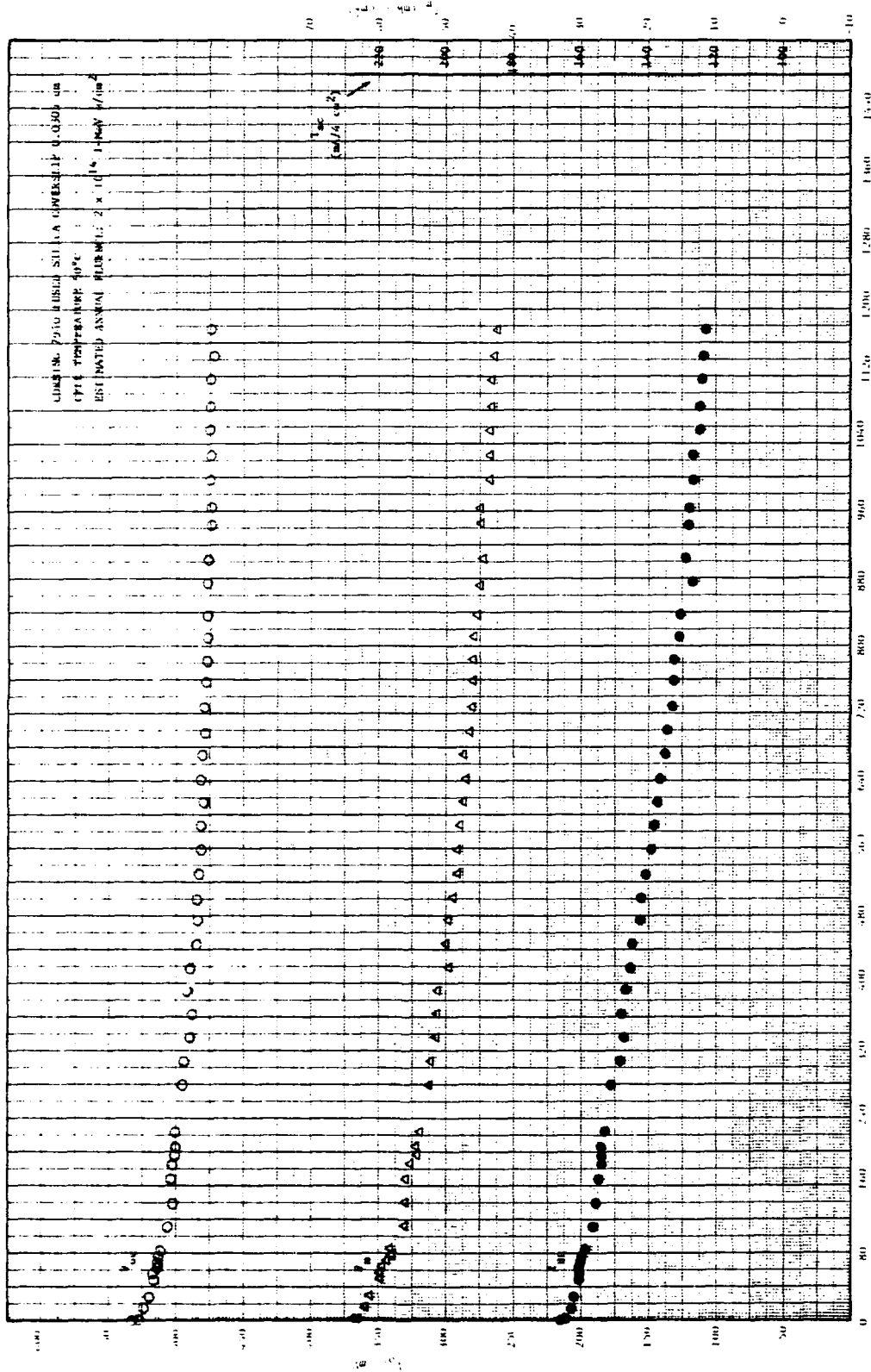
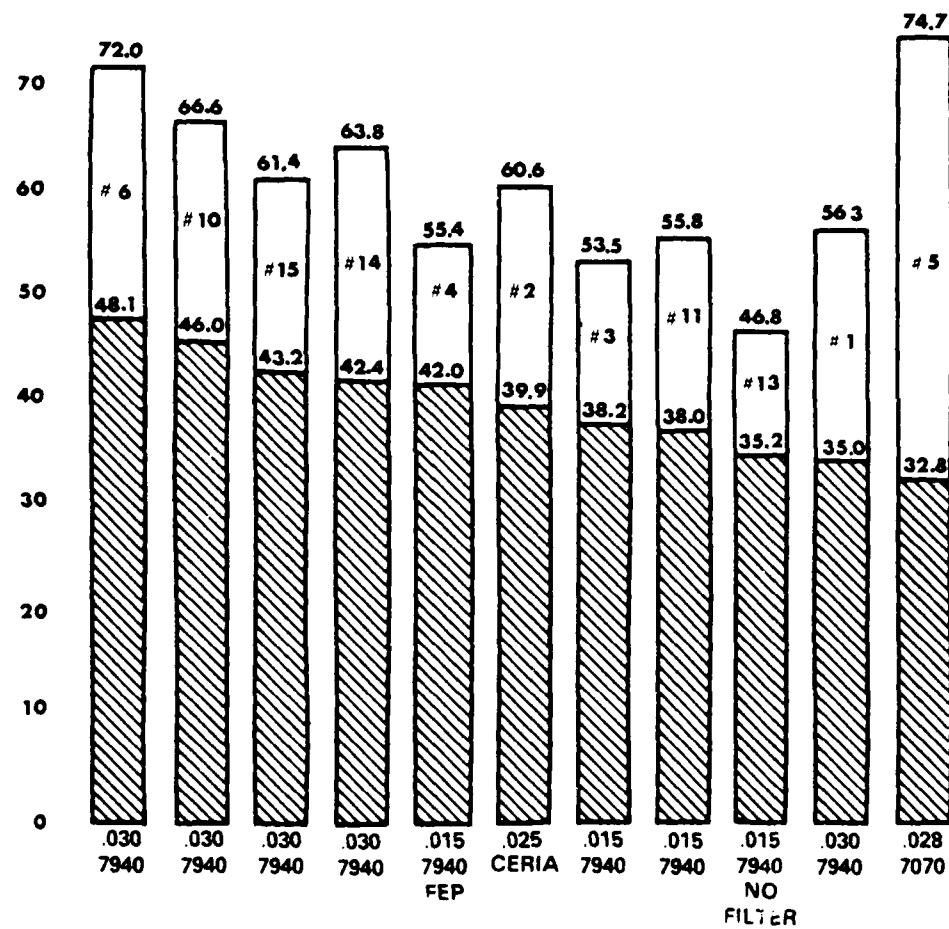


Fig. 26 — Degradation of  $P_m$ ,  $I_{sc}$  and  $V_{oc}$  of the Spectrolab HESP solar cell.  
 $I_{sc}$  and  $P_m$  are normalized to  $4 \text{ cm}^2$ . (Experiment 14).

×2 CELL TEMPERATURE IS 50°C)



COVERSIDE MATERIAL AND THICKNESS (cm)

Fig. 27 — Maximum power of solar cell modules after 1,176 days in orbit

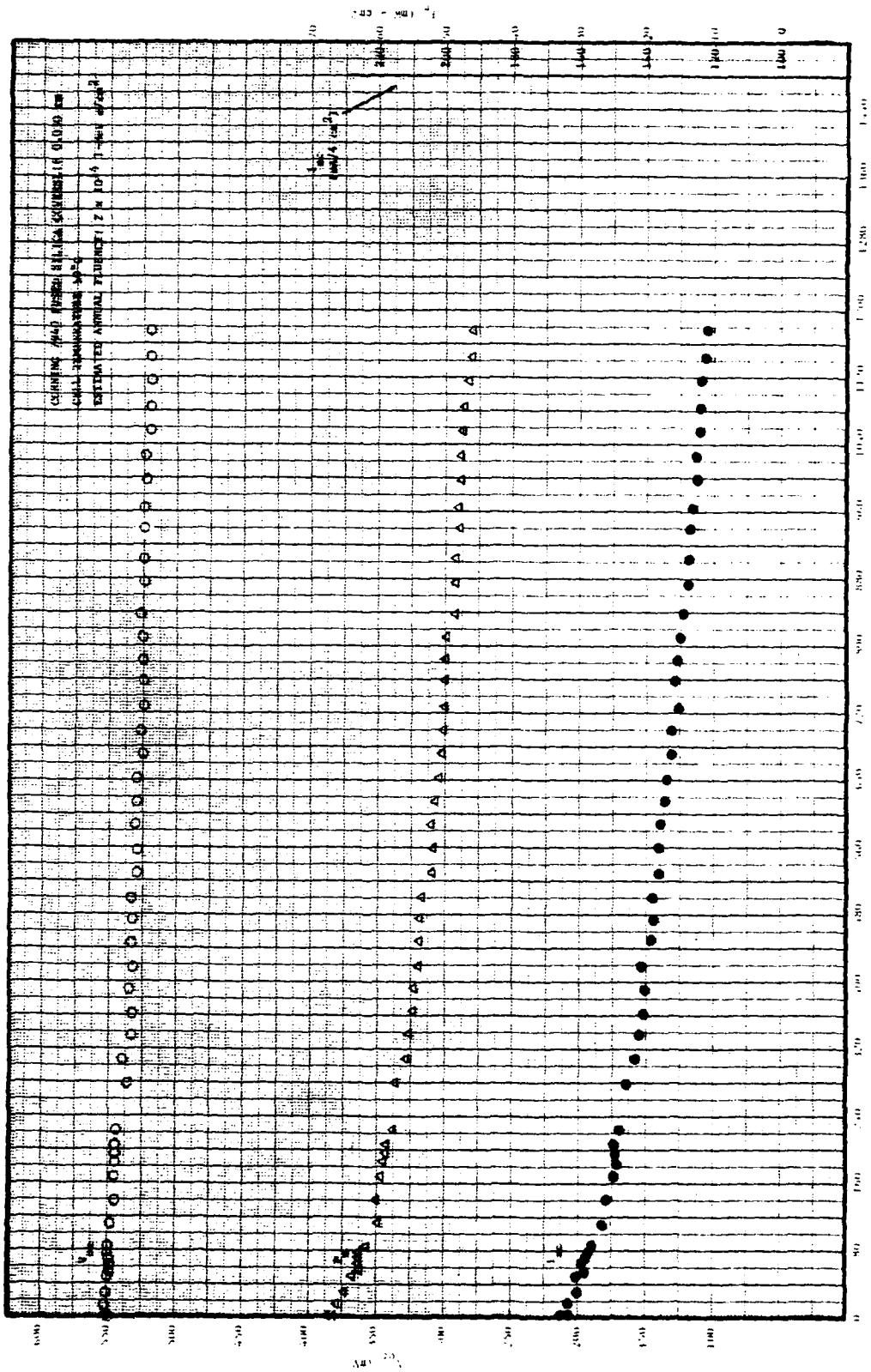


Fig. 28 — Degradation of  $P_m$ ,  $I_{sc}$  and  $V_{oc}$  of the OCL1 violet.  $P_m$  and  $I_{sc}$  are normalized to  $4 \text{ cm}^2$ . (Experiment 10).

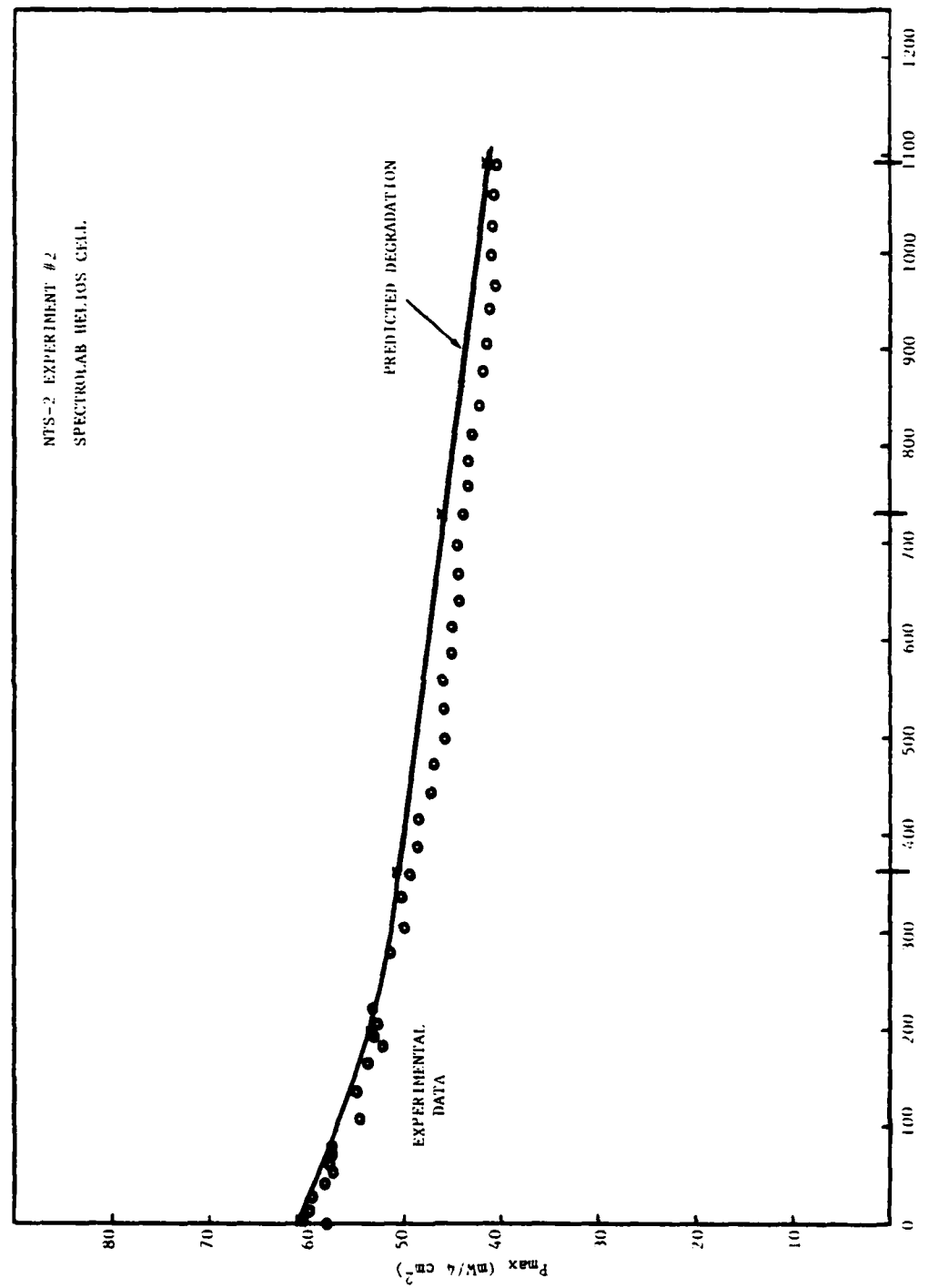


Fig. 29 — Predicted degradation rate for the Spectrolab Helios cell over a three-year period.  
Cell temperature is 50°C.

Table I – NTS-2 Solar Cell Experiments

Exp. No.	Cell Type	Thickness (cm)	Covership (cm)	Covership Bond (cm)	Interconnect	Efficiency 28°C (%)
1	OCLI Conventional, 2 ohm-cm	0.025	Corning 7940, AR and UV, (0.030)	R63-489	Cu/Ag	10.7
2	Spectrolab "Helios" p <sup>+</sup> 15-45 ohm-cm	0.0228	Ceria microsheet w/o AR, (0.025)	DC 93-500	Moly/Ag (.0025)	11.5
3	Spectrolab Hybrid Sculptured 7-14 ohm-cm	0.020	Corning 7940, AR and UV, (0.0152)	DC 93-500	Moly/Ag (.0025)	10.5
4	Spectrolab Hybrid Sculptured 7-14 ohm-cm	0.020	Corning 7940, w/o AR or UV, (0.0152)	FEP Teflon (0.0051)	Moly/Ag (.0025)	11.1
5	Comsat Non-Reflecting, p <sup>+</sup> Textured, 1.8 ohm-cm	0.025	Corning 7940, AR, w/o UV (.030)	R63-489	Ag; thermo-compression bonding	14.5
6	Comsat Non-Reflecting, p <sup>+</sup> Textured, 1.8 ohm-cm	0.025	Corning 7940, AR and UV (.030)	R63-489	Ag; thermo-compression bonding	14.6
7	Solarex Vertical Junction, p <sup>+</sup> , 1.5 ohm-cm	0.030	Ceria microsheet w/o AR (.0152)	Sylgard 182	Ag mesh	13.0
8	Solarex Space Cell, p <sup>+</sup> 2 ohm-cm	0.025	Ceria microsheet w/o AR (0.0152)	Sylgard 182	Ag mesh	12.8
9	Spectrolab "Helios" p <sup>+</sup> Sculptured, BSR, 10 ohm-cm	0.030	Corning 7940 (.030)	FEP teflon (.003)	Ag mesh (.003)	14.2
10	OCLI Violet, 2 ohm-cm	0.025	Corning 7940 (.030)	R63-489	Cu/Ag	13.5
11	Spectrolab P/N Li-doped 15-30 ohm-cm, Al contacts	0.020	Corning 7940, AR and UV, (0.015)	Silicone	Aluminum (.0025) Ultrasonic welding	10.8
12	Spectrolab P/Planar Diode in series with Exp. 11	NA	NA	NA	NA	NA
13	OCLI Conventional, 2 ohm-cm	0.025	Corning 7070 (.028)	Electrostatic bonding	Cu/Ag	10.2
14	Spectrolab HESP, no p <sup>+</sup> , Sculptured, 2 ohm-cm	0.030	Corning 7940, AR and UV (0.0305)	R63-489	Moly/Ag (.00025)	13.6
15	Hughes Gallium-Aluminum Arsenide	0.0305	Corning 7940, AR and UV, (0.0305)	DC 93-500	Aluminum GPD (.00025), epoxy	13.6

TABLE II  
NTS-2 MAXIMUM POWER OUTPUT FOR SOLAR CELL EXPERIMENTS

MAXIMUM POWER OUTPUT (mW/4 cm<sup>2</sup>)\*

EXPERIMENT NO.	CELL TYPE	SOLAR SIMULATOR	DAY 1 IN ORBIT	DAY 1176 IN ORBIT	% LOSS DAY 1 TO DAY 1176
1	OCLI Conv. 2 ohm-cm	53.1	56.3	35.0	37.8
2	Spectrolab Helios (NTS-2)	57.9	60.6	39.9	34.2
3	Spectrolab Text. Hybr., F.S.	52.4	53.5	38.2	28.6
4	Spectrolab Text. Hybr., FEP, F.S. w/o filter	54.6	55.4	42.0	24.2
5	Comsat Text. F.S., w/o filter	72.8	74.7	32.8	56.1
6	Comsat Text. F.S.	70.1	72.0	48.1	33.2
7	Solarex Vert. Junc.	63.1	62.2	(Module Failed on Day 759)	
8	Solarex Space Cell	60.6	63.1	(Module Failed on Day 69)	
9	Spectrolab Text. Helios Reflector	66.0	70.0	(Module Failed on Day 783)	
10	OCLI Violet, F.S.	67.5	66.6	46.0	30.9
11	Spectrolab HASP w/o diode	53.2	55.8	38.0	31.9
12	Spectrolab HASP w/diode	42.0	42.1	26.8	36.3
13	OCLI Conv., ESB	47.0	46.8	35.2	24.8
14	Spectrolab HESP	63.3	63.8	42.4	33.5
15	HRL AlGaAs	70.0	61.4	43.2	29.6

\*These data have been corrected to 50°C at one-sun and air mass zero (AM0).

TABLE III  
NTS-2 SHORT-CIRCUIT CURRENT OUTPUT FOR SOLAR CELL EXPERIMENTS

EXPERIMENT NO.	CELL TYPE	SOLAR SIMULATOR	SHORT-CIRCUIT CURRENT OUTPUT (mA/4 cm <sup>2</sup> )*		
			DAY 1 IN ORBIT	DAY 1176 IN ORBIT	% LOSS DAY 1 TO DAY 1176
1	OCLI Conv. 2 ohm-cm	135.4	136.5	93.3	31.6
2	Spectrolab Helios (NTS-2)	154.5	155.5	115.0	26.0
3	Spectrolab Text. Hybr., F.S.	155.6	154.0	117.0	24.0
4	Spectrolab Text. Hybr., FEP, F.S. w/o filter	151.0	149.6	125.5	16.1
5	Comsat Text. F.S., w/o filter	184.8	180.4	91.2	49.4
6	Comsat Text. F.S.	180.8	178.7	126.6	29.2
7	Solarex Vert. Junc.	158.4	160.5	(Module Failed on Day 759)	
8	Solarex Space Cell	155.9	158.8	(Module Failed on Day 69)	
9	Spectrolab Text. Helios Reflector	174.3	175.8	(Module Failed on Day 783)	
10	OCLI Violet, F.S.	165.1	164.3	122.2	25.6
11	Spectrolab HASP w/o diode	136.2	132.6	106.1	20.0
12	Spectrolab HASP w/diode	134.5	132.4	105.9	20.0
13	OCLI Conv., ESB	147.3	146.1	121.7	16.7
14	Spectrolab HESP	166.2	165.8	123.2	25.7
15	HRL AlGaAs	102.9	100.6	71.3	29.1

\*These data have been corrected to 50°C at one-sun and air mass zero (AM0).

TABLE IV  
NTS-2 OPEN-CIRCUIT VOLTAGE OUTPUT FOR SOLAR CELL EXPERIMENTS\*

EXPERIMENT NO.	CELL TYPE	SOLAR SIMULATOR	DAY 1 IN ORBIT	DAY 1176 IN ORBIT	% LOSS DAY 1 TO DAY 1176
1	OCLI Conv. 2 ohm-cm	533	549	504	8.2
2	Spectrolab Helios (NTS-2)	527	546	477	12.6
3	Spectrolab Text. Hybr., F.S.	491	508	476	6.1
4	Spectrolab Text. Hybr., FEP, F.S. w/o filter	491	505	472	6.5
5	Comsat Text. F.S., w/o filter	533	555	496	10.6
6	Comsat Text. F.S.	533	549	504	8.2
7	Solarex Vert. Junc.	528	521	(Module Failed on Day 759)	
8	Solarex Space Cell	535	541	(Module Failed on Day 69)	
9	Spectrolab Text. Helios Reflector	550	545	(Module Failed on Day 783)	
10	OCLI Violet, F.S.	550	552	519	6.0
11	Spectrolab HASP w/o diode	552	559	519	7.2
12	Spectrolab HASP w/diode	523	523	478	8.6
13	OCLI Conv., ESB	488	490	451	8.0
14	Spectrolab HESP	533	528	474	10.2
15	HRL AlGaAs	914	895	853	4.7

\*These data have been corrected to 50°C at one-sun and air mass zero (AM0).

TABLE V  
NTS-2 SOLAR CELL EXPERIMENTS  
SUMMARY OF CHANGES IN PHOTOVOLTAIC PARAMETERS\*

EXPERIMENT NO.	CELL TYPE	PERCENT LOSS DAY 1 TO DAY 1176		
		MAXIMUM POWER	SHORT-CIRCUIT CURRENT	OPEN-CIRCUIT VOLTAGE
1	OCLI Conv. 2 ohm-cm	37.8	31.6	8.2
2	Spectrolab Helios (NTS-2)	34.2	26.0	12.6
3	Spectrolab Text. Hybr., F.S.	28.6	24.0	6.1
4	Spectrolab Text. Hybr., FEP, F.S. w/o filter	24.2	16.1	6.5
5	Comsat Text. F.S., w/o filter	56.1	49.4	10.6
6	Comsat Text. F.S.	33.2	29.2	8.2
7	Solarex Vert. Junc.	(Module Failed on Day 759)		
8	Solarex Space Cell	(Module Failed on Day 69)		
9	Spectrolab Text. Helios Reflector	(Module Failed on Day 783)		
10	OCLI Violet, F.S.	30.9	25.6	6.0
11	Spectrolab HASP w/o diode	31.9	20.0	7.2
12	Spectrolab HASP w/diode	36.3	20.0	8.6
13	OCLI Conv., ESB	24.8	16.7	8.0
14	Spectrolab HESP	33.5	25.7	10.2
15	HRL AlGaAs	29.6	29.1	4.7

\*These data have been corrected to 50°C at one-sun and air mass zero (AM0).

Table VI — NTS-2 Equivalent Fluence (1 - MeV e/cm<sup>2</sup>) Predictions\*

OCLI Conventional 2 Ω-cm, 10 mil cell, 12 mil FS Coverslip

BOL		Fluence at 200 days	Fluence at 1 yr	Fluence at 3 yr
$I_{sc}$	136.0 mA	$1.5 \times 10^{14}$	$2.7 \times 10^{14}$	$8.2 \times 10^{14}$
$V_{oc}$	548 mV	$3 \times 10^{13}$	$5.5 \times 10^{13}$	$1.6 \times 10^{14}$
$P_m$	56.5 mW/4 cm <sup>2</sup>	$1.3 \times 10^{14}$	$2.4 \times 10^{14}$	$7.1 \times 10^{14}$
Spectrolab Helios, 10 Ω-cm, 9 mil cell, 10 mil Ceria Coverslip				
BOL		Fluence at 200 days	Fluence at 1 yr	Fluence at 3 yr
$I_{sc}$	154 mA	$1.3 \times 10^{14}$	$2.4 \times 10^{14}$	$7.1 \times 10^{14}$
$V_{oc}$	545 mV	$1 \times 10^{13}$	$1.8 \times 10^{13}$	$5.5 \times 10^{13}$
$P_m$	60.5 mW/4 cm <sup>2</sup>	$9 \times 10^{13}$	$1.6 \times 10^{14}$	$4.9 \times 10^{14}$
Spectrolab Textured Hybrid, 8 mil cell, 6 mil FS Coverslip				
BOL		Fluence at 200 days	Fluence at 1 yr	Fluence at 3 yr
$I_{sc}$	156 mA	$5.0 \times 10^{14}$	$9.1 \times 10^{14}$	$2.7 \times 10^{15}$
$V_{oc}$	522 mV	$5.0 \times 10^{14}$	$9.1 \times 10^{14}$	$2.7 \times 10^{15}$
$P_m$	53.8 mW/4 cm <sup>2</sup>	$3.3 \times 10^{14}$	$6.0 \times 10^{14}$	$1.8 \times 10^{15}$
OCLI Violet				
BOL		Fluence at 200 days	Fluence at 1 yr	Fluence at 3 yr
$I_{sc}$	166 mA	$1 \times 10^{13}$	$1.8 \times 10^{14}$	$5.5 \times 10^{14}$
$V_{oc}$	552 mV	$2 \times 10^{13}$	$3.7 \times 10^{13}$	$1.1 \times 10^{14}$
$P_m$	67.5 mW/4 cm <sup>2</sup>	$7.5 \times 10^{13}$	$1.4 \times 10^{14}$	$4.1 \times 10^{14}$

\*Cell data at 50°C

Table VII -- Percent of  $I_{sc}$ ,  $V_{oc}$  and  $P_{max}$  Remaining after 200 Days in Orbit  
and Predictions for Percent Remaining at 1 yr and 3 yrs\*

OCLI Conventional, 2  $\Omega$ -cm, 10 mil cell, 12 mil FS Coverslip

BOL		Relative Degradation at 200 days	Relative Degradation at 1 yr	Relative Degradation at 3 yrs
$I_{sc}$	136.0 mA	.91	.87	.81
$V_{oc}$	548 mV	.98	.97	.94
$P_m$	56.5 mW/4 cm <sup>2</sup>	.87	.82	.75

Spectrolab Helios, 10  $\Omega$ -cm, 9 mil cell, 10 mil Ceria Coverslip

BOL		Relative Degradation at 200 days	Relative Degradation at 1 yr	Relative Degradation at 3 yrs
$I_{sc}$	154 mA	.95	.91	.87
$V_{oc}$	545 mV	.98	.96	.93
$P_m$	60.5 mW/4 cm <sup>2</sup>	.88	.84	.76

Spectrolab Textured Hybrid, 8 mil cell, 6 mil FS Coverslip

BOL		Relative Degradation at 200 days	Relative Degradation at 1 yr	Relative Degradation at 3 yrs
$I_{sc}$	156 mA	.93	.90	.82
$V_{oc}$	522 mV	.96	.94	.90
$P_m$	53.8 mW/4 cm <sup>2</sup>	.90	.87	.74

OCLI Violet, 10 mil cell, 12 mil FS Coverslip

BOL		Relative Degradation at 200 days	Relative Degradation at 1 yr	Relative Degradation at 3 yrs
$I_{sc}$	166 mA	.90	.84	.80
$V_{oc}$	552 mV	.98	.97	.95
$P_m$	67.5 mW/4 cm <sup>2</sup>	.87	.83	.75

\*Cell data at 50°C

### References

1. W. Luft, "Effects of Electron Irradiation on N-on-P Silicon Solar Cells," Advanced Energy Conversion, Vol. 5, pp. 21-41 (1965).
2. J.A. Martin, et al., "Radiation Damage to Thin Silicon Solar Cells," IECEC Advanced in Energy Conversion Engineering (Intersociety Energy Conversion Engineering Conf.), pp. 289-296 (1967).
3. R.L. Statler, "One MeV Electron Damage in Silicon Solar Cells," Proc. 1968 IECEC, pp. 122-127.
4. J.L. Goldhammer and B.E. Anspaugh, "Electron Spectrum Irradiations of Silicon Solar Cells," Proc. Eighth IEEE Photovoltaic Specialists Conf., pp. 201-208 (1970).
5. D.J. Curtin and A. Meulenberg, "Statistical Analysis of One MeV Electron Irradiation of Silicon Solar Cells," Proc. Eighth IEEE Photovoltaic Specialists Conf., pp. 193-300 (1970).
6. R.L. Crabb, "Photon Induced Degradation of Electron and Proton Irradiated Silicon Solar Cells," Tenth IEEE Photovoltaic Specialists Conf. Rec., pp. 396-403, 1974.
7. W. Luft, "Radiation Effects on High Efficiency Silicon Solar Cells," Evaluation De L'Action De L'Environnement Spatial Sur Les Materiaux, Colloque International, Toulouse, June 1974, p. 627.
8. D.J. Curtin and R.L. Statler, "Review of Radiation Damage to Silicon Solar Cells," IEEE Transactions on Aerospace and Electronic Systems, Vol. AES-11, No. 4, July 1975, pp. 499-513.
9. L.J. Goldhammer, "Particulate Irradiations of an Advanced Silicon Solar Cell," Conf. Record of the Eleventh IEEE Photovoltaic Specialists Conf., Scottsdale, AZ, 6-8 May 1975.
10. W. Luft, "Radiation Effects on High Efficiency Silicon Solar Cells," IEEE Transactions on Nuclear Science, Vol. NS-23, No. 6, Dec. 1976, pp. 1795-1802.

- II. R.L. Statler and F.C. Treble, "Solar Cell Experiments on the TIMATION III Satellite," Proc. of the International Conf. on Photovoltaic Power Generation, Hamburg, Germany, 25-27 Sep. 1974, pp. 369-377.
12. R.L. Statler and D.H. Walker, "Solar Cell Experiments on the NTS-1 Satellite, Conf. Record of the Eleventh IEEE Photovoltaic Specialists Conf., Scottsdale, AZ, 6-8 May 1975, pp. 190-193.
13. R.L. Statler, D.H. Walker and R.J. Lambert, "The NTS-1 Solar Cell Experiment After Two Years in Orbit," Conf. Record of the Twelfth IEEE Photovoltaic Specialists Conf., Baton Rouge, LA, 15-18 Nov 1976.
14. W.P. Rahilly, Air Force Aero Propulsion Laboratory, private communication.
15. J.F. Allison, Comsat Laboratories, private communication.
16. R. Obenschain, P. Pierce, P. Hyland and R. Rasmussen, "The Revised Solar Array Synthesis Computer Program," RCA Final Report, NAS-5-11669 for NASA Goddard Space Flight Center, 1 Feb 1970.
17. H.Y. Tada and J.R. Carter, Jr., "Solar Cell Radiation Handbook," Pasadena, CA; Jet Propulsion Lab., JPL Pub. 77-56, November 1977.
18. E.G. Stassinopoulos, "Charged Particle Radiation Environment for NTS-2 and NTS-3 Satellites," NASA Goddard Space Flight Center, X-601-80-1, 1979.

DATE  
ILME